 doi:10.20944/preprints202204.0097.v1

Review

Post-proline cleaving enzymes (PPCEs): Classification, structure, molecular properties, and applications

Anis Baharin[1†], Tiew-Yik Ting[2†], Hoe-Han Goh[3*]

[1] Institute of Systems Biology, Universiti Kebangsaan Malaysia, UKM Bangi 43600 Selangor, Malaysia; anis.baharin@gmail.com
[2] Institute of Systems Biology, Universiti Kebangsaan Malaysia, UKM Bangi 43600 Selangor, Malaysia; ting-tiewyik@gmail.com
[3] Institute of Systems Biology, Universiti Kebangsaan Malaysia, UKM Bangi 43600 Selangor, Malaysia; gohhh@ukm.edu.my
† These authors have contributed equally to this work and share the first authorship
* Correspondence: gohhh@ukm.edu.my; Tel.: +603-8921-4557

Abstract: Proteases or peptidases are hydrolases that catalyze the breakdown of polypeptide chains into smaller peptide subunits. Proteases exist in all life forms, including archaea, bacteria, protozoa, insects, animals, and plants, due to their vital functions in cellular processing and regulation. There are several classes of proteases in the MEROPS database based on their catalytic mechanisms. This review focuses on the post-proline cleaving enzymes (PPCEs), especially the prolyl endoprotease/oligopeptidase (PEP/POP). To date, most PPCEs studied are of microbial and animal origins. Recently, there are reports of new plant PPCEs. The most common PEP/POP are members of the S9 family that comprise two conserved domains. The substrate-limiting β-propeller domain prevents unwanted digestion, while the α/β hydrolase catalyzes reaction at the carboxyl-terminal of proline residues. PPCEs have diverse applications, are widely used in the beer brewing industry, and have potential as therapeutic agents for Alzheimer's disease and celiac disease by targeting proline-rich substrates. Protein engineering via mutagenesis has been performed to improve heat resistance, pepsin-resistant capability, specificity, and protein turnover of PPCEs for pharmacological applications. This is the first comprehensive review to cover the biotechnological applications of PPCEs and discuss the unique prolyl cleaving activity of different enzymes based on the recent structure-function studies from diverse taxa.

Keywords: Prolyl endoprotease; prolyl oligopeptidase; protease; protein engineering; proteolytic enzyme; proteomics; therapeutics

1. Introduction

Peptidases, proteases, proteinases, or proteolytic enzymes break down peptide molecules, mostly by attacking peptide bonds via hydrolysis. Extensive protease studies found seven main catalytic types, which can be categorized by the nucleophiles for the proteolytic reaction with water molecules. The nucleophiles mainly comprise different amino acid residues, including aspartate, cysteine, glutamate, serine, threonine, and whilst another type contains metal ions (mostly zinc) at their active site, denoted as metalloproteases [1]. The seventh catalytic type performs intramolecular self-cleavage without water molecules using asparagine as a nucleophile [2]. Besides catalytic type, proteases can be further classified according to the peptide cleavage sites between the amino (N-) and carboxyl (C-) termini of proteins, such as aminopeptidase, carboxypeptidase, endopeptidase, or exopeptidase [3]. An oligopeptidase only cleaves peptides but not proteins. As of March 2022, there were 281 protein families in the MEROPS peptidase database, comprising 4,431 peptidases with identifiers, which were classified into nine cata-

 doi:10.20944/preprints202204.0097.v1

lytic types aspartic (A, 324), cysteine (C, 1,059), glutamic (G, 22), metallo (M, 1,098), asparagine (N, 24), mixed (P, 54), serine (S, 1,728), threonine (T, 105), and unknown/unclassifiable (U, 17).

This review will focus on the post-proline cleaving enzymes (PPCEs), especially prolyl endoprotease/oligopeptidase (PEP/POP). Many PPCEs can be found in the MEROPS peptidase database from over 17 families with different substrates and proline-cleavage specificities (Table 1). This list of PPCEs is mostly dominated by the serine protease (S) family, including S06, S09, S15, S28, S33, and S37 with nucleophilic serine residue for catalysis [4]. Both PEP and POP hydrolyze polypeptides at the C-terminal of proline residues (Pro-Xaa) with PEP not restricted by protein size, while POP can only cleave small peptides [5]. Studies have shown that different PEPs can cleave a 33-mer gliadin peptide from wheat and synthetic peptides at different rates for different species [6,7]. Apart from the serine protease family S9, the metalloprotease families M12 and M13 are also overrepresented with subfamilies possessing the post-proline cleaving (PPC) activity (Table 1). The term PPCEs in this review is used to encompass other proteins with PPC activity beyond the serine protease family. To date, reports of PPCEs from plants are relatively scarce compared to extensive studies of PPCEs in microbes and animals (Table 2).

The purpose of this review is to discuss recent findings on the molecular mechanism of PPCEs based on the structure-function analysis. The biochemical properties, such as substrate specificity and optimal conditions of enzymatic activity were summarized for both the native and recombinant PPCEs from the recent experimental findings. Lastly, the utilization of PPCEs for different applications in proteomics, the food/beer brewing industry, and pharmaceuticals/therapeutics will be described.

Preprints (www.preprints.org) | NOT PEER-REVIEWED | Posted: 11 April 2022 doi:10.20944/preprints202204.0097.v1

Table 1. A non-exhaustive list of selected enzymes with post-proline cleaving activity based on records from the MEROPS peptidase database release 12.4.

Family	Subfamily	Peptidase	UniProt / MEROPS ID	Specificity†	Substrate	Cleavage Site	Reference
G3 [1/1]	G03.001	Strawberry mottle virus glutamic peptidase	MER1365461	2/2 (100%)	Polyprotein	Peptide-Pro↓Ala/Lys-Peptide	[8]
M2 [4/7]	M02.003	Peptidyl-dipeptidase angiotensin-converting enzyme (ANCE)	Q10714/ MER0001987	6/7 (86%)	Bradykinin	Peptide-Pro↓Phe/Tyr-Arg	[9]
	M02.006	Angiotensin-converting enzyme-2	Q9BYF1/ MER0011061	10/14 (71%)	Angiotensin-2	Peptide-Pro↓Phe	[10]
M3 [8/11]	M03.002	Neurolysin	P42676/ MER0001942	68/128 (53%)	Neurotensin	Peptide-Pro↓Tyr-Peptide	[11]
M9D [1/2]	M9D.002	Proline-specific peptidyl-dipeptidase (*Streptomyces*)	-	2/2 (100%)	Leu-Pro-Pro-Pro-Pro-Pro	Leu-Pro-Pro-Pro↓Pro-Pro	[12]
M12 * [41/109]	M12.164	Lebetase	Q98995/ MER0002591	6/14 (43%)	Bradykinin	Peptide-Pro↓Phe-Arg	[13]
	M12.338	BmooMPalpha-I (*Bothrops* sp.)	P85314/ MER0104668	21/36 (58%)	Bradykinin	Peptide-Pro↓Phe-Arg	[14]
M13 * [11/13]	M13.005	Oligopeptidase O3 (PepO)	MER0001059	3/7 (43%)	Beta-casein	Peptide-Pro↓Val/Ile-Peptide	[15]
	M13.010	Oligopeptidase O2 (PepO)	O52071/ MER0004645	4/4 (100%)	Beta-casein	Peptide-Pro↓Val/Ile-Peptide	[16]
M34 [3/3]	M34.002	Pro-Pro endopeptidase 1 (*Clostridium difficile*-type)	MER0494994	13/13 (100%)	Putative adhesin	Peptide-Asn-Pro↓Pro-Peptide	[17]
	M34.003	Pro-Pro endopeptidase 2	MER0328914	3/3 (100%)	Putative s-layer protein	Peptide-Pro↓Pro-Peptide	[18]
M64 [1/1]	M64.001	IgA peptidase (*Clostridium ramosum*-type)	MER0016067	2/2 (100%)	Immunoglobulin IgA1	Peptide-Pro↓Val-Peptide	[19]
M72 [2/2]	M72.002	CpaA g.p. (*Acinetobacter baumannii*)	MER1365492	2/2 (100%)	Coagulation factor XII	Peptide-Pro↓Thr-Peptide	[20]
S6 [4/8]	S06.001	IgA1-specific serine peptidase (*Neisseria*-type)	MER0000278	6/6 (100%)	Immunoglobulin IgA1	Peptide-Pro↓Xaa-Peptide	[21]
	S06.007	IgA1-specific serine peptidase type 1 (*Haemophilus* sp.)	MER0001759	3/3 (100%)	IgA1 chain C region	Peptide-Pro↓Thr-Peptide	[22]
S9 * [21/32]	S09.001	Prolyl oligopeptidase	P23687/ MER0000392	50/59 (85%)	Alpha/beta-gliadin MM1	Peptide-Pro↓Xaa-Peptide	[23]
	S09.002	Prolyl oligopeptidase homologue (*Pyrococcus*-type)	MER0000398	2/3 (67%)	Z-Gly-Pro-NHPhNO2	Z-Gly-Pro↓NHPhNO2	[24]
	S09.003	Dipeptidyl-peptidase IV (eukaryote)	P27487/ MER0000401	21/29 (72%)	C-X-C motif chemokine 10	Val-Pro↓Leu-Peptide	[25]
	S09.006	Dipeptidyl aminopeptidase B (fungus)	P18962/ MER0000405	5/7 (71%)	Alanyl/prolyl bond	Xaa-Ala/Pro↓Xaa	[26]
	S09.007	Fibroblast activation protein alpha subunit	Q12884/ MER0000399	6/6 (100%)	Alpha-2-antiplasmin	Peptide-Pro↓Asn/Leu-Peptide	[27]

Preprints (www.preprints.org) | NOT PEER-REVIEWED | Posted: 11 April 2022 doi:10.20944/preprints202204.0097.v1

	S09.008	Dipeptidyl peptidase 4 (*Aspergillus*-type)	MER0004504	6/8 (75%)	[Des-Arg]-bradykinin	Pro-Pro↓Gly-Peptide	[28]
	S09.009	Dipeptidyl-peptidase 4 (bacteria-type 1)	Q5NMM8/ MER0041840	3/5 (60%)	Gly-Pro-NHNap	Gly-Pro↓NHNap	[29]
	S09.013	Dipeptidyl-peptidase 4 (bacteria-type 2)	Q47900/ MER0001423	15/17 (88%)	Beta-casein	Tyr-Pro↓Phe-Peptide	[30]
	S09.017	Prolyl tripeptidyl peptidase	Q7MUW6/ MER0005196	13/13 (100%)	Cystatin C	Ser-Ser-Pro↓Gly-Peptide	[31]
	S09.018	Dipeptidyl-peptidase 8	Q6V1X1/ MER0013484	8/10 (80%)	C-X-C motif chemokine 10	Val-Pro↓Leu-Peptide	[32]
	S09.019	Dipeptidyl-peptidase 9	Q86TI2/ MER0004923	13/15 (87%)	RU1 antigenic peptide	Val-Pro↓Tyr-Peptide	[33]
	S09.033	Prolyl oligopeptidase (zoomastigote)	Q4E132/ MER0079308	-	-	-	[34]
	S09.036	Rv0457C peptidase (*Mycobacterium tuberculosis*)	MER0003229	2/2 (100%)	Suc-Gly-Pro-NHMec	Peptide-Pro↓NHMec	[35]
	S09.073	Xaa-Pro dipeptidylpeptidase	D7UPN5/ MER0195666	19/19 (100%)	Ala-Pro-NHPhNO2	Xaa-Pro↓NHPhNO2	[36]
	S09.076	Prolyl oligopeptidase (*Myxococcus xanthus*)	Q9X5N2/ MER0005694	2/2 (100%)	Suc-Ala-Pro-NHPhNO2	Peptide-Pro↓NHPhNO2	[37]
	S09.077	Prolyl oligopeptidase B (*Galerina marginata*)	H2E7Q8/ MER0325901	3/3 (100%)	Alpha-amanitin proprotein 1	Peptide-Pro↓Ile/Trp-Peptide	[38]
	S09.UPA	Subfamily S9A unassigned peptidases	-	3/3 (100%)	Gly-Pro-NHPhNO2	Gly-Pro↓NHPhNO2	[39]
S15 [1/1]	S15.001	Xaa-Pro dipeptidyl-peptidase	Q02W78/ MER0000443	8/10 (80%)	Gly-Pro-NHPhNO2	Gly-Pro↓NHPhNO2	[40]
S28 [2/3]	S28.001	Lysosomal Pro-Xaa carboxypeptidase	P42785/ MER0000446	11/11 (100%)	Endothelin B receptor-like protein 2	Peptide-Pro↓Ala	[41]
	S28.004	Acid prolyl endopeptidase (*Aspergillus* sp.)	A2QR21/ MER0093133	-	-	-	[42]
S33 [5/10]	S33.001	Prolyl aminopeptidase	P42786/ MER0000431	4/6 (67%)	Consensus prolyl bond	Pro↓Xaa	[43]
	S33.004	Prolyl dipeptidase (*Lactobacillus*-type)	A8YWX2/ MER0000437	17/18 (95%)	Pro-Gly	Pro↓Xaa	[44]
	S33.008	Prolyl aminopeptidase 2	P46547/ MER0001367	9/10 (90%)	Pro-NHPhNO2	Pro↓NHPhNO2	[45]
S37 [1/1]	S37.001	PS-10 peptidase	Q54408/ MER0001350	3/3 (100%)	Transglutaminase precursor	Pepetide-Pro↓Asp-Peptide	[46]
U9G [3/20]	U9G.029	Prolyl endopeptidase (*Spinacia*)	-	3/3 (100%)	Oxygen-evolving enhancer protein 3, chloroplastic	Peptide-Pro↓Ile/Leu-Peptide	[47]
U74 [1/1]	U74.001	Neprosin	-	51/110 (46%)	Alpha/beta-gliadin MM1	Peptide-Pro↓Xaa-Peptide	[48]

 doi:10.20944/preprints202204.0097.v1

↓: cleavage site; -: the linked amino acids; NA: not available; Xaa: any amino acid.

ǂSpecificity is based on the MEROPS specificity matrix showing the proportion of proline residue in the P1 cleavage site of all substrate cleavage records.

Numbers in square brackets indicate the proportion of subfamily with records of post-proline cleavage. * Overrepresented (P<0.001) based on the hypergeometric test.

Table 2. The post-proline cleaving enzymes that are reported in the different species discussed in this review.

Taxa	Species (common name)	UniProt / PDB ID	MEROPS	Enzyme	Reference
Virus	Strawberry Mottle Virus	- / -	G03.001	Glutamic peptidase	[8]
Archaea	*Pyrococcus furiosus*	Q51714 / 5T88	S09.002	POP	[49]
Bacteria	*Aeromonus punctata*	Q9X6R4 / 3IUM	S09.001	PEP	[50]
	Flavobacterium meningosepticum	P27195 / -	S09.UPA	POP	[51]
	Lactobacillus helveticus	O52071 / -	M13.010	PepO-3	[16]
	Meiothermus ruber H328	A0A7C3HT26 / -	S09.UPA	PEP/POP	[39]
	Mycobacterium tuberculosis	O07178 / -	S09.036	POP	[35]
	Myxococcus xanthus	Q9X5N2 / 2BKL	S09.076	POP	[37]
	Porphyromonas gingivalis	Q7MUW6/2D5L	S09.017	PTP	[52]
	Serratia marcescens	O32449 /1QTR	S33.001	PAP	[53]
	Sphingomonas capsulate	Q9ZNM8 / -	S9.UPA	POP	[37]
	Stenotrophomonas maltophilia	A0A0U5BDB7/-	S9.UPW	PEP	[54]
Fungi	*Aspergillus niger*	A2QR21 / 7WAB	S28.004	AN-PEP	[42]
	Aspergillus oryzae	A0A1S9DCM9 / -	S28.004	PEP	[55]
	Galerina marginata	H2E7Q8 / 5N4C	S09.077	POP-B	[38]
Protozoa	*Trypanosoma brucei*	Q6HA27 / -	S09.033	POP	[56]
	Trypanosoma cruzi	Q71MD6 / -	S09.033	POP	[57]
Insects	*Drosophila melanogaster*	Q10714 / 2X91	M02.003	ANCE	[58]
	Eurygaster integriceps (sunn pest)	E1U339 / -	S09.001	PEP	[6]
	Haematobia irritans (buffalo fly)	Q10715 / -	M02.003	PDP	[9]
Animals	*Haliotis discus* (abalone)	A0A1X9T5X9 / 6JYM	S09.UPA	PEP	[59]
	Homo sapiens	P48147 / 3DDU	S09.001	POP	[60,61]
		P27487 / 1J2E	S09.003	DPP-IV	[62]
		P42785 / 3N2Z	S28.001	Lysosomal PRCP	[63]
		Q9BYF1 / 1R42	M02.006	ACE-2	[64]
	Mus musculus (mouse)	P42676 / 1I1I	M03.002	Neurolysin (POP)	[65]
		Q9QUR6 / -	S09.001	POP	[66]
	Bothrops sp. (snake)	P85314 / 3GBO	M12.338	BmooMPalpha-I	[14]
	Sus scrofa (porcine)	P23687 / 1O6G	S09.001	POP	[67]

 doi:10.20944/preprints202204.0097.v1

Plants	*Arabidopsis thaliana*	F4HSS5 / -	S33.001	PAP	[63]
	Coffea arabica (coffee)	- / -	S09.001	POP	[68]
	Daucus carota (carrot)	- / -	S09.UPA	PEP	[69]
	Nepenthes sp. (pitcher plant)	A0A1V0DK55 / -	U74.001	Neprosin	[70]
	Secale cereale × *Triticum turgidum subsp. durum*	G9J616 / -	S33.001	PAP	[71]
	Spinacia oleracea (spinach)	P12301 / -	U9G.029	PEP	[72]
	Vigna radiata (mung bean)	-	S28.002	DPP-II	[73]

*****ACE/ANCE: angiotensin-converting enzyme; DPP: dipeptidyl-peptidase; PAP: prolyl aminopeptidase; PDP: peptidyl-dipeptidase; PEP: prolyl endoproteinase; PepO: oligopeptidase O; POP: prolyl oligopeptidase; PRCP: Pro-Xaa carboxypeptidase; -: not available

Italic PDB ID indicates the crystal structure for the homology modeling in SWISS-MODEL.

Preprints (www.preprints.org) | NOT PEER-REVIEWED | Posted: 11 April 2022 doi:10.20944/preprints202204.0097.v1

2. Molecular structure and biochemistry

2.1 Structural studies

Protein structures of PPCEs have been studied across different taxa including fungus, bacteria, animals, and plants (Table 2). The protein structures found in the PDB database are mostly solved through x-ray crystallography. The first crystal structure for a prolyl oligopeptidase (POP) was solved in 1998 at 1.4 Å resolution to reveal the α/β hydrolase fold and β-propeller domains with a catalytic triad of Ser-His-Asp [67]. Subsequently, crystal structures were acquired for *Sphingomonas capsulate* (1.8 Å resolution) and *Myxococcus xanthus* (1.5 Å resolution)[37].

Based on the sequence alignments and structural models, POP proteins from the MEROPS S9 family have two conserved domains (Figure 1). The C-terminal catalytic α/β-hydrolase domain comprises an alpha/beta/alpha sandwich for protein cleaving, whereas the N-terminal β-propeller domain constitutes β-sheets that limit proteolysis to smaller substrates as a mechanism to avoid non-targeted digestion [37,50,74]. The electron microscopy of human PEP revealed the presence of a new side opening that was not observed in any of the crystallographic structures [74]. Two paths were identified using the CAVER algorithm, leading from the PEP active site to the outside solvent, one through the β-propeller and another one through a large side aperture into the catalytic domain [74].

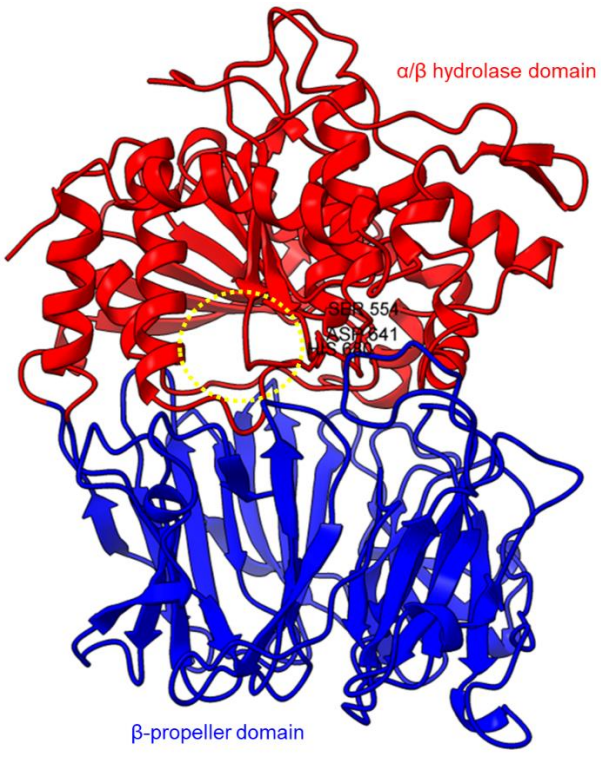

Figure 1. Crystal structure of a porcine POP (PDB ID: 1QFM). In red is the α/β hydrolase catalytic domain, whereas the β-propeller domain is highlighted in blue. Catalytic triad residues: Ser554, Asp641, and His680 are labeled. The yellow circle indicates a probable accessible path discovered in an electron microscopy study [74].

Preprints (www.preprints.org) | NOT PEER-REVIEWED | Posted: 11 April 2022 doi:10.20944/preprints202204.0097.v1

PEP/POP from different species have different β-propeller sizes, thus conferring specificity to different sizes of substrates targeting proline residues that are usually resistant to protein cleavage by other peptidases [75,76]. For example, studies on *Arabidopsis thaliana*, *Homo sapiens*, and *Sus scrofa* (porcine) showed that each POP possesses a unique affinity toward different sizes of ligands despite high sequence and structural similarities [77]. Besides the pore size of β-propellers, the number of β-propeller blades also plays a role in the substrate specificity of PEP. For instance, the porcine POP (S9a, S09.001) has a seven-bladed β propeller structure that acts as a filtering gate to exclude large peptides from the active site [67]; whereas the crystal structure of the human dipeptidyl-peptidase (DPP IV) (S9b, S09.003) shows a unique eight-bladed β-propeller (Figure 2). The irregular blade-1 on DPP-IV is hypothesized to allow substrate entry to the catalytic site without going through the gating filter compared to POP [62]. The difference in the β-propeller of POP and DPP-IV could have contributed to the substrate specificity of these two enzymes in which POP hydrolyses small peptides (<30 amino acids) at the C-terminal of proline residues, while DPP-IV cleaves dipeptides at the penultimate proline residue. As compared to the β-propeller domains, the α/β-hydrolase catalytic domain is mostly conserved.

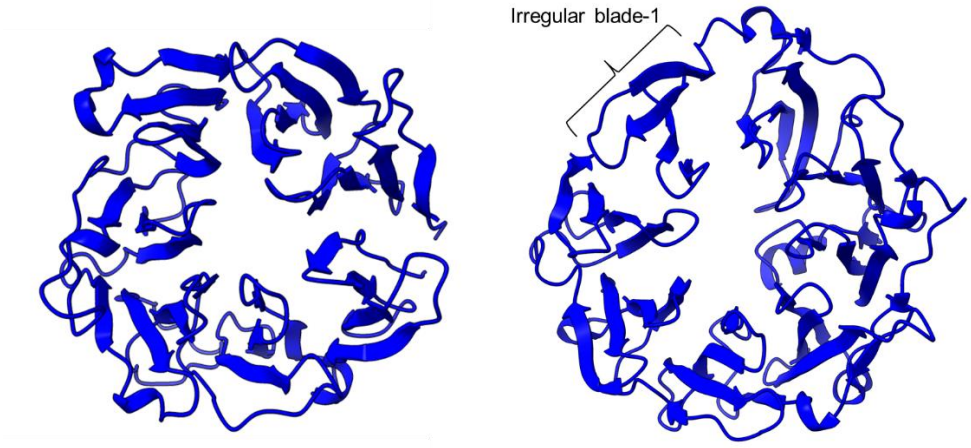

Figure 2. The β-propeller structure of a porcine prolyl oligopeptidase POP (PDB id: 1QFM, left) and a human dipeptidyl peptidase DPP-IV (PDB ID: 1J2E, right). The labeled irregular blade-1 of the eight-blade β-propeller structure could contribute to different substrate specificity between POP and DPP-IV.

There is a recent report of the *Aspergillus niger* PEP (AN-PEP) structure solved through x-ray crystallography [78]. AN-PEP belongs to the peptidase family S28 of Pro-Xaa carboxypeptidase, which is in the same SC clan with family S9 sharing the same catalytic site residues (Ser-Asp-His) and likely the same evolutionary origin. The AN-PEP structure consists of 17 α-helices, ten 310 helices, and ten β-strands. In contrast to the POP of peptidase family S9, the β-propeller domain is replaced by a helical SKS domain (Figure 3) that is stabilized by three disulfide bonds. The catalytic pocket of AN-PEP is located between the catalytic α/β hydrolase domain and the SKS domain. AN-PEP is capable of digesting large substrates, unlike POP with a substrate limit of less than 30 amino acids. The substrate specificity could be due to the differences in the catalytic pocket structure formed between the α/β hydrolase and SKS domains in AN-PEP, compared to the β-propeller domain of S9 PEP/POP.

Preprints (www.preprints.org) | NOT PEER-REVIEWED | Posted: 11 April 2022 doi:10.20944/preprints202204.0097.v1

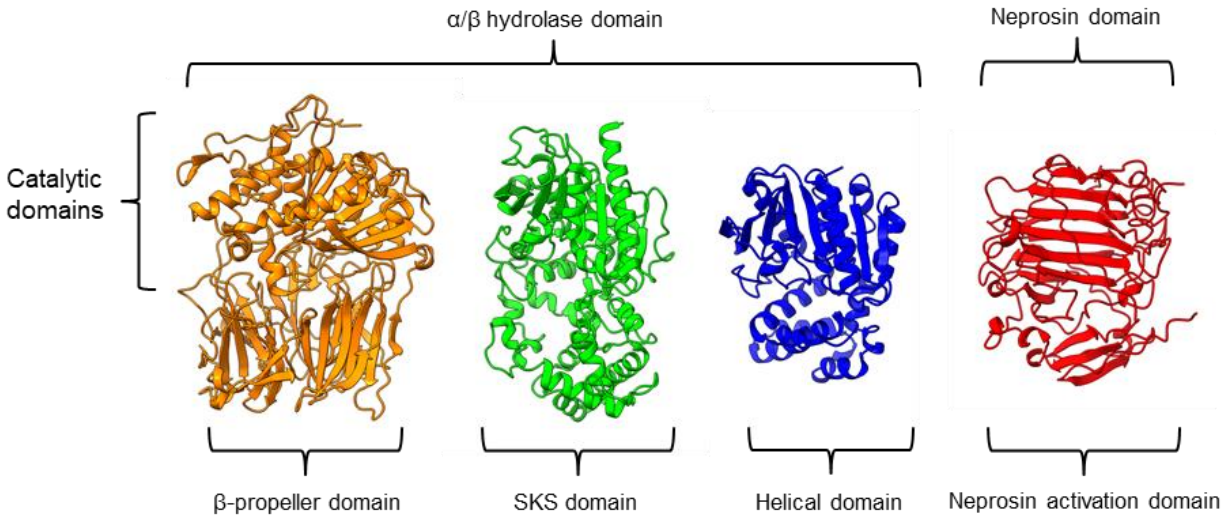

Figure 3. Representative protein structures from MEROPS peptidase family S9 (porcine muscle prolyl oligopeptidase, PDB ID: 1QFM), S28 (*Aspergillus niger* prolyl endoprotease, PDB ID: 7WAB), S33 (*Serratia marcescens* prolyl aminopeptidase, PDB ID: 1QTR), and U74 (AlphaFold2 model of *N.* × *ventrata* neprosin, NvNpr), from left to right. The three-dimensional protein structures are oriented with their catalytic domains on top.

Another family of PPCEs is the prolyl aminopeptidase (PAP) from the peptidase family S33 that can be found in the apricot seeds [77] and cabbage leaves [79]. Prolyl aminopeptidase (S33.001) is an exopeptidase that catalyzes the removal of the proline residue at the N-terminal of a peptide [53]. Similar to peptidase families S9 and S28, the catalytic α/β hydrolase domain is present (Figure 3). However, it has a catalytic triad of Ser113, His296, and Asp 268 with a consensus sequence of GXSXG around the catalytic serine residue. The second unannotated helices domain comprises six α-helices that act as a cap to block the N-terminal of the pre-cleavage (P1) proline, thus explaining the exopeptidase catalytic mechanism. PAPs are categorized based on their functioning structures: 30-35 kDa monomers (S33.001) are found exclusively in bacteria, while 100-370 kDa multimers (S33.008) have been reported in bacteria, fungi, and plants. Interestingly, a biochemically characterized plant PAP from *Triticosecale* is more similar to the monomeric PAPs than the multimeric form [76].

On the other hand, a protease from the carnivorous tropical pitcher plants known as neprosin with PPC activity was classified as an unknown peptidase family (U74). There is a recent neprosin structure-function analysis based on the AlphaFold2 modeling that suggests neprosin belongs to the glutamic peptidase family with two glutamic acid residues as the catalytic dyad [80]. Unlike the S9, S28, or S33 prolyl proteases, neprosin does not have an α/β hydrolase domain, SKS domain, or β-propeller domain. Instead, neprosin has two uncharacterized domains, namely the neprosin activation domain and the neprosin domain (Figure 3). The neprosin domain is proposed to be the catalytic domain due to the absence of the neprosin activation domain in the active enzyme either in the native or recombinant neprosins [48,81]. Intriguingly, the neprosin domain comprises predominantly β-sheets, which form two antiparallel six- and seven-stranded β-sheets with an overall β-sandwich structure.

PPC activity was also reported in a few members of zinc metallopeptidase families (M2, M3, M9D, M12, M13, M34, M64, and M72). Peptidyl-dipeptidase ANCE (M02.003), angiotensin-converting enzyme-2, ACE2 (M02.006), and neurolysin (M03.002) comprise two domains annotated as zinc metallopeptidase domain I and domain II [64,65,82]. An active channel with a bound zinc ion is located in between the two active helices domains

Preprints (www.preprints.org) | NOT PEER-REVIEWED | Posted: 11 April 2022 doi:10.20944/preprints202204.0097.v1

connected by small secondary structures (Figure 4). One of the structural differences between ACE2 and neurolysin is the number of the strand of the β-sheet on domain II, where ACE2 has a three-stranded β-sheet while neurolysin has a five-stranded β-sheet (Figure 4). Furthermore, the more flexible loop structures on neurolysin could have contributed to its wide substrate specificity [65].

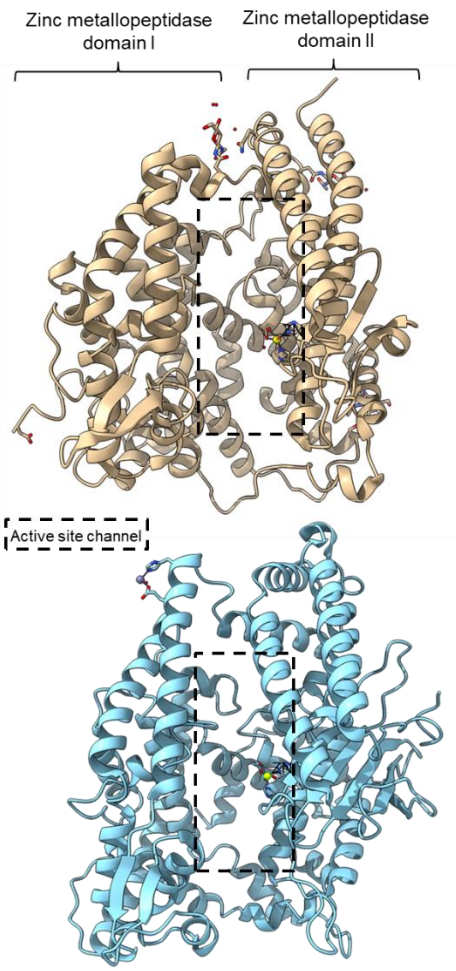

Figure 4. Crystal structures of the MEROPS metallopeptidase M02.006 angiotensin-converting enzyme-2, ACE2 (top, PDB ID: 1R42), and M03.002 neurolysin (bottom, PDB ID: 1I1I).

Metallopeptidase M12 BmooMPalpha-I (M12.338, 3gbo) with a molecular mass of 22.6 kDa has conserved features of P-I class snake venom metallopeptidases, namely the five-stranded β-sheet, four long helices, and a short α-helix near N-terminal stabilized by three disulfide bridges [14]. The zinc ion is bound to three histidine residues: His140, His144, and His150 (Figure 5). Besides, Pro-Pro endopeptidase 1, PPEP-1 (M34.002, 5a0p), and Pro-Pro endopeptidase 2, PPEP-2 (M34.003, 6fpc) shared a very similar structure with an α/β N-terminal domain (NTD) comprising twisted four-stranded β-sheet and three α-helices (α1-α3), and an α C-terminal domain (CTD) with four α-helices (α5-α8) [18,83]. The active site of Pro-Pro endopeptidase 2 is located at the α4-helix that separates NTD and CTD domains. A zinc ion is bound to the catalytic base Glu138, two histidine residues (His137 and His141) from α4-helix, Tyr174 from α5/α6-helices, and Glu181 from α6-helix (Figure 5). The four amino acids substrate loops (S-loops) in PPEP-1 (GGST) and PPEP-2 (SERV) are shown to contribute to the difference in their substrate specificities [18]. Therefore, peptidases with proline-cleaving activity are not confined to the serine peptidase family alone. The advent of accurate ab initio protein structure prediction from sequences will reveal more peptidases conferring PPC activity via different catalytic mechanisms

Preprints (www.preprints.org) | NOT PEER-REVIEWED | Posted: 11 April 2022 doi:10.20944/preprints202204.0097.v1

with different structures and provide a further understanding of the structure-function of the PPCEs.

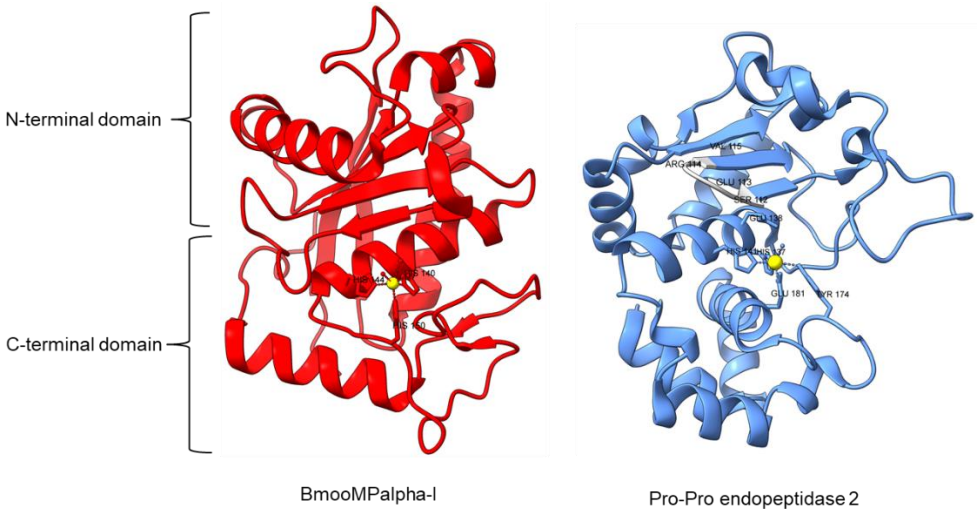

Figure 5. Crystal structures of MEROPS metallopeptidase M12.338 BmooMPalpha-I (left, PDB ID: 3GBO) and M34.003 Pro-Pro endopeptidase 2 (right, PDB ID: 6FPC) with substrate loop (S-loop) SERV in light gray. The zinc ions are shown as yellow spheres.

2.2 Molecular mechanisms of PPCEs

Typically, PEP/POP from the clan SC of family S9 comprises a catalytic triad with the following order, Ser-Asp-His with the catalytic Ser lies in between the Gly-X-Ser-X-Gly motif [67]. However, there are also "nonclassical" serine proteases such as the Ser/His/Glu, Ser/His/His, and Ser/Glu/Asp triads, Ser/Lys and Ser/His dyads, and even peptidases with a single serine catalyst [84]. For S9 PEP, two major hypotheses on substrate binding mechanism had been proposed. The initial hypothesis is that the substrate enters the filtering gate and the central channel formed by the β-propeller structure before reaching the active site. This theory is supported by *Sphingomonas capsulate* PEP as it failed to digest the 33-mer substrate (LQLQPFPQPQLPYPQPQLPYPQPQLPYPQPQPF) effectively with a diameter larger than the 4 Å channel formed by the β-propeller domain. However, this theory cannot explain why S9 PEP from *Myxococcus xanthus and Flavobacterium meningosepticum* can digest the 33-mer substrate in the same study. Later, it is proposed that substrate binding with the β-propeller domain induces conformation changes, causing the domain to move and expose the active site. This theory is supported by the open state of *Sphingomonas capsulate* PEP structure, where an opening of 30 Å is observed between the α/β hydrolase and β-propeller domain [37].

Another study obtained an open state of *Aeromonus punctata* PEP and proposed an induced-fit mechanism as the conformational changes in the PEP can be induced by adding substrate and inhibitor [50]. The open state is achieved when the substrate H2H3 is added, while a close state occurs after the binding of the Z-prolyl-prolinal (ZPP) inhibitor with PEP (Figure 6). HP35 substrate with over 30 amino acids can enter the active site but is not cleaved as the catalytic residue is not in an active conformation in the open state; whereas the catalytic pocket with the active catalytic triad conformation in a close state is too small for HP35. Recently, a molecular simulation of *Pyrococcus furiosus* POP (S09.002) shows that the conformational change is modulated by the "latching loop" mechanism, and is essential for the catalysis mechanism of POP, especially for the loop containing catalytic histidine residue (H592) [49]. The conformation of the histidine loop during the shifting of open to close state allows H592 to move closer to the active site for the catalytic triad formation. Chloride ion binding is required for the loop movement with subsequent activation of the POP peptidase catalysis.

Preprints (www.preprints.org) | NOT PEER-REVIEWED | Posted: 11 April 2022 doi:10.20944/preprints202204.0097.v1

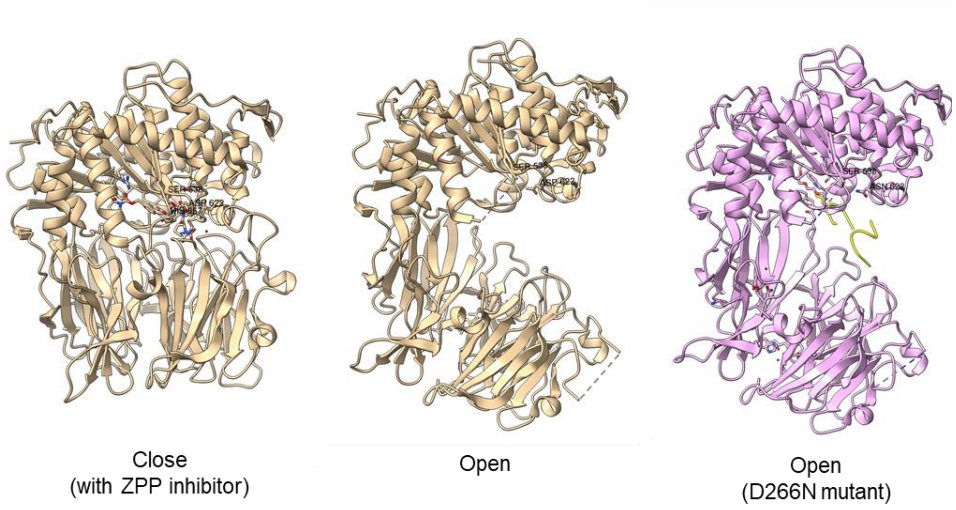

Figure 6. Crystal structures of *Aeromonas punctata* PEP (ApPEP). From left to right: close-state wild type ApPEP with ZPP inhibitor (PDB ID: 3IVM), open-state wild type ApPEP (PDB ID: 3IUL), mutant ApPEP with D266N mutation in an open state (PDB ID: 3IUR) induced by two H2H3 substrates (yellow). The catalytic triad (Ser538, Asp622, and His657) are labeled. However, the loops containing histidine catalytic residue (His657) are missing in the open-state crystal structures as they are unresolved in electron density maps and are inherently flexible.

For peptidase family S28, it is suggested that the difference in the catalytic pocket located between α/β hydrolase and SKS domain could confer substrate specificity based on the recent AN-PEP crystal structure [78]. The catalytic pocket formed in AN-PEP is wide-open compared to lysosomal Pro-Xaa carboxypeptidase (PRCP) (S28.001) and dipeptidyl peptidase II, DPP7 (S28.002) with a volume-limited catalytic pocket that will affect the recognition of substrates with different sizes [63]. However, the residues such as Glu88, Pro205, Trp374, and Trp460 are conserved across PEP, PRCP, and DPP7 despite differences in the volumes of catalytic pocket.

Different from S9 and S28 families, the S33 family has exopeptidase properties whereby it cleaves the proline residues at the N-terminal of a peptide. Prolyl aminopeptidase from *Serratia marcescens* (S33.001) has a similar α/β hydrolase domain and another smaller helical domain made up of six helices which are smaller than the SKS domain on S28. The smaller domain of prolyl aminopeptidase is believed to contribute to the exopeptidase specificity of S33 prolyl protease as the specificity hydrophobic pocket is formed on the helices domain [53]. Two mutagenesis studies on prolyl aminopeptidase from *Serratia marcescens* concur that residues Phe139, Tyr149, and Glu204 play important role in substrate recognition [85,86]. Phe139, Tyr149, and Phe236 in the hydrophobic pocket together with Glu204 and Glu232 are involved in the electrostatic interactions. The proline recognition is completed by four electrostatic interactions and the insertion of substrate into the hydrophobic pocket of prolyl aminopeptidase [85]. Substrate acetylation could help in the orientation of the substrate in the active cleft for efficient hydrolysis [87]. The catalytic mechanism of peptidase family S28 and S33 could be like that of S9 prolyl endopeptidase as they shared a similar classical serine catalytic triad of Ser-Asp-His.

Other than serine peptidases, a glutamic peptidase was reported with PPC activity and a catalytic dyad comprising two catalytic glutamic acid residues [8]. *In silico* analysis of neprosin found a high structural similarity to strawberry mottle virus glutamic peptidase (SMoV peptidase, G03.001) with the overlapping catalytic dyad [80]. This shed light on the possible catalytic mechanism of neprosin. The mature neprosin has a putative accessible active cleft formed by the β-sandwich structure for substrate binding. The catalytic mechanism of glutamic peptidase G3 could be like that of the Gln and Glu catalytic

Preprints (www.preprints.org) | NOT PEER-REVIEWED | Posted: 11 April 2022 doi:10.20944/preprints202204.0097.v1

dyad in the G1 family because the main catalytic Glu residue of glutamic peptidase G1 is found to be conserved in the G3 family [88].

2.3 Biochemical studies of PPCEs

The native and recombinant proteins of PPCEs have been reported for different species, mainly microbes, and animals. PEP can decompose various hard-to-degrade proteins with different preferences towards different amino acids surrounding the proline residues. For example, the recombinant PEP from a gram-negative thermophile, *Meiothermus ruber* H328 shows more flexibility in terms of preferences towards the second and third residues near proline, but stringent preference towards residues next to proline [39].

Studies on both the native and recombinant PPCEs, mainly PEP/POP, showed similar optimum temperatures with pH 4-6, except for *Eurygaster integriceps*, *Haliotis discus*, *Sus sucrofa*, *Porphyromonas gingivalis*, and *Nepenthes* × *ventrata* (Tables 3 and 4). The majority of the native protein studies were based on *Aspergillus niger* with pH 4-5 and 37 °C. Nearly all recombinant protein characterization studies used *Escherichia coli* as a cloning and expression host apart from *Pichia pastoris* and wheat (Table 4). Some PPCEs exhibited different preferences for different substrate lengths and specificity with a broad range of optimum temperatures and pH levels. For instance, a POP (S09.001) cleaves after the C-terminal proline residue in peptide substrates with less than 30 amino acids.

In addition to the PPC activity that cleaves at two conserved prolines of α-amanitin pro-peptide, POP-B from *Galerina marginata* (GmPOPB, S09.077) has a unique transpeptidation activity that catalyzes macrocyclization of a 25-mer peptide to form a monocyclic octapeptide [38]. A PEP from *Aspergillus oryzae* (S28.004) exhibits a similar PPC activity at an optimal pH of 2.5 with the capability of digesting much larger substrates such as intact casein [89]. Similar to S28 PEP, neprosin with a lower molecular mass (~30 kDa) shows PPC activity at pH 2.5 but with no limitation of substrate size [81]. Prolyl aminopeptidase (S33.001) from family S33 has a proline-specific exopeptidase activity which cleaves proline at the N-terminal of a peptide [53]. All PPCEs showed the ability to cleave proline-rich substrates. These studies suggest the potential of PPCEs from different species to be used in various conditions of pH and temperature for industrial applications.

 doi:10.20944/preprints202204.0097.v1

Table 3. The optimum conditions of selected native PPCEs in substrate degradation.

Source	Enzyme	Substrate*	pH	T (°C)	Method to detect digested substrate*	Reference
Fungus						
Aspergillus niger	PEP	Beer hordein	-	-	ELISA RIDASCREEN® Gliadin competitive	[90]
			4–5	-	Gluten ELISA assay	[91]
			-	14	Antibody-based competitive enzyme-linked immunosorbent assay	[92]
			4	37	Gluten ELISA assay	[93]
			4.6	37	Western blot, monoclonal antibody-based competition assays	[94]
			4–5	37	SDS-PAGE, Western blot, ELISA, HPLC, MS,	[95]
		Wheat flour, gliadin	4	40	ELISA, immunoblot (anti-PEP-I, anti-PEP-II, and anti-HMW-GS antibodies), RP-HPLC	[7]
		N-glycosidase	4–4.5	37	MALDI-TOF MS	[96]
		ZGPpNA	4	37	Turbidity (protein-polyphenol haze)	[97]
			4–5	40–50	UV-Vis 410 nm	[98]
Insect						
Eurygaster integriceps (sunn pest)	PEP	ZGPpNA	8 & 10	24–34	UV-Vis 410 nm	[6]
Animal						
Mus musculus	POP	Suc-Gly-Pro-AMC	4.2	30	Fluorescence plate reader	[66]
Plants						
Nepenthes × *ventrata*	Neprosin	α-gliadin	2.5	37	SDS-PAGE, turbidity monitored at 595 nm, MS/MS	[48]
Spinacia oleracea PSII membranes	PEP	Co-purified 23 kDa and 18 kDa proteins	6	37	Densitogram	[72]
Vigna radiata	DPP-II	-4mβNA & -βNA dipeptides	7.5	37	UV-Vis 520 nm	[73]

* -4mβNA: -4-methoxy-β-naphthylamide; -βNA: -beta-naphthylamide; ELISA: enzyme-linked immunosorbent assay; -4mβNA: -methoxy-β-naphthylamide; MS: mass spectrometry; MS/MS: tandem MS; RP-HPLC: reversed-phase high-performance liquid chromatography; NA: not available; SDS-PAGE: sodium dodecyl sulfate-polyacrylamide gel electrophoresis; ZGPpNA: benzyloxycarbonyl-Gly-Pro-p-nitroanalide

 doi:10.20944/preprints202204.0097.v1

Table 4. The optimum conditions of selected recombinant PPCEs in substrate degradation.

Source	Enzyme	Expression host	Expression	Purification	Substrate	pH	T (°C)	Assay detection	Reference
Fungi									
Aspergillus niger	AN-PEP	*Pischia pastoris* GS115/pPIC9K	28°C/96 h	Ni-affinity chromatography	ZGPpNA	4–5	35–40	UV-Vis 410 nm	[89]
							35	LC-MS/MS	[99]
Aspergillus oryzae	Prolyl aminopeptidase	*Escherichia coli* BL21/pET-28a(-)	25°C/12 h	Ni-affinity chromatography	L-Pro-pNA	6.5-7.5	50	-	[100]
Bacteria									
Flavobacterium meningosepticum	Fm-POP	Wheat/pUC57	-	-	Gluten peptide	6	37	HPLC, ELISA	[51]
		E. coli DH5α/pUC57+Fmen	37°C/14 h	Geneclean III kit	ZGPpNA, gliadin, glutenin	-	Up to 90	UV-Vis	[101]
Meiothermus ruber H328	MrPEP	*E. coli* BL21(DE3)/pET-28b	37°C/14 h	DEAE-cellulose & Phenyl-FF chromatography	ZGPpNA, suc-Ala-Pro-*p*NA, Gly-Pro-*p*NA, Pro-*p*NA	9	60	UV-Vis, FRETS-25Xaa libraries, LC-MS	[39]
Myxococcus xanthus	PEP	*E. coli* BL21(DE3)/pET-28b	22°C/16 h	Ni-affinity chromatography	Collagen peptide	6–7	36 –37	UV-HPLC-MS/MS	[77]
Porphyromonas gingivalis	Prolyl tripeptidyl aminopeptidase	*E. coli* M15/pQE30-ptpA	30°C/18 h	Butyl-sepharose column	Fluorogenic substrate	7.5	30	UV-Vis	[52]
Sphaerobacter thermophiles	PEP	*E. coli* DE3/pET-15b	37°C/24 h	Ni-NTA resin spin column	ZGPpNA, gluten peptide	6.6	63	Enzymatic assay, MS	[102]
Sphingomonas capsulate	PEP	*E. coli* BL21(DE3)/pET-28b	22°C/16 h	DEAE & Blue sepharose chromatography	Chromogenic Gluten peptide	6–7	36 –37	UV-HPLC-MS/MS	[77]
Insect									
Eurygaster integriceps	PEP	*E. coli* BL21(DE3)/pNYCO	28°C/16 h	Ni-affinity chromatography	ZGPpNA, wheat gluten	7.5	37	UV-Vis	[103]

Preprints (www.preprints.org) | NOT PEER-REVIEWED | Posted: 11 April 2022 doi:10.20944/preprints202204.0097.v1

Haematobia irritans exigua	ANCE	-	-	Lectin-affinity & ion-exchange chromatography	Angiotensin 1, cholecystokinin-8	7.5	37	HPLC	[9]
Animals									
Haliotis discus (abalone)	PEP	*E. coli* BL21(DE3)	18°C/15 h	Ni-affinity chromatography	Collagen peptide	6	20	HPLC-MS	[37]
Sus sucrofa	POP	*E. coli* Top10/pBAD	37°C/4-6 h	DEAE and Blue sepharose chromatography	ZGPpNA -AMC	5–8	30	UV-Vis	[104]
Plant									
Nepenthes × *ventrata*	Neprosin	*E. coli* Arctic Express/pET-28a(+)	16°C/16 h	Ni-affinity chromatography	HeLa cell protein	2.5	37–50	MS	[81]
					Histone	2.5	37	LC-MS/MS	[105]

* AMC: 7-amido-4-methylcoumarin; DEAE: diethylaminoethyl; ELISA: enzyme-linked immunosorbent assay; Hb: hemoglobin; HPLC: high-performance liquid chromatography; L-Pro-pNA: L-arginyl-L-proline 4-nitroanilide; MS: mass spectrometry; Ni-NTA: Ni^{2+}-nitrilotriacetate; UV-Vis: ultraviolet-visible spectroscopy; ZGPpNA: Z-Gly-Pro-4-nitroanilide; - : not available

 doi:10.20944/preprints202204.0097.v1

3. Biological functions of PPCEs

3.1 Microbes and Protozoa

Many PPCEs are found in microbes that have been purified and characterized. The strawberry mottle virus glutamic peptidase unit (G03.001) can cleave at P↓AFP sites of the coat protein domain in the polyprotein and is hypothesized to be involved in the regulatory step of controlling viral RNA encapsidation [8]. Proline iminopeptidase or proline aminopeptidase (PAP) from family S33, including *Flavobacterium meningosepticum* and *Serratia marcescens* (S33.001), could be involved in pathogenicity by breaking down peptides rich in proline and hydroxyproline such as collagen [87]. Rv0457c peptidase (S09.036) from the S9 family is a POP found in *Mycobacterium tuberculosis* that can stimulate the secretion of proinflammatory cytokines by peritoneal macrophage and lead to inflammatory response during *M. tuberculosis* infection [35]. Besides, POP-B of *Galerina marginata* (S09.077) from the same family is required for the maturation of α-amanitin, a toxin that is responsible for the fatal mushroom poisoning [38]. There is also a proline-Xaa carboxypeptidase (AoS28D, S28.004) from *Aspergillus* sp. with different biochemical properties than the other paralogs from gene duplication, which functions together with other secreted aminopeptidases and carboxypeptidases to digest large peptides for uptake [106].

On the other hand, the POP zoomastigote (S09.033) from the unicellular parasitic flagellate protozoa *Trypanosoma cruzi* and *T. brucei* are involved in the pathophysiology of Chagas disease and human African trypanosomiasis, respectively [57]. The *Trypanosoma* spp. attached to the extracellular matrix (ECM) releases POPs that degrade collagen. The entry of *Trypanosoma* spp. with degraded collagen peptides signal host leukocytes to release matrix metalloproteases (MMPs) that further break down the ECM barrier. Ultimately, this allows the parasite to break through protective barriers such as ECM or blood-brain barrier in causing diseases. These examples demonstrate that microbial and protozoa PPCEs have diverse biological roles, many of which are important in pathogenicity.

3.2 Animals

PPCEs have been associated with diverse physiological roles in animals, especially humans. In mice, POP (S09.001) was highly expressed in the brain, kidney, testis, and thymus with the kidney having the least enzymatic activity [66]. Moreover, POP was also found in the mouse peripheral tissues and placental extract showing that it might have important functions in these regions. An immunohistochemistry study has unveiled high POP densities in the caudate nucleus and putamen, hippocampus, and cortex [107]. POP activities are widespread but cell-specific in peripheral tissues, especially the secreting epithelial cells in the stomach, breast ducts, kidney, pancreas, and reproductive system [61]. Like mice, a high amount of POP is detected in the human testis, particularly in nuclei of primary spermatocytes and spermatids, oocytes, and primary follicles. Furthermore, POP is found to be elevated especially in malignant tumors [61].

PPCEs appear to play an important role in memory and learning as well as cognitive and behavioral development. For example, alterations of POP and dipeptidyl-peptidase IV (DPP-IV, S09.003) levels in different brain parts were observed in mice of different genders administered with DPP-IV inhibitor [108]. Other than the localization of POP in the brain, the distribution of POP in the human brain resembled that of inositol 1,4,5-triphosphate (IP3) receptors, which supports that POP plays a role in movement regulation, cognition, and IP3 signaling [107]. High POP activity in the human cortex suggests a role in memory, cognition, and learning. Altered POP activities were found in patients suffering from cognitive diseases and other health implications. Increased PEP activity is associated with inflammation [109] as well as mania and schizophrenia [110], whereas decreased POP activity is related to depression [111], multiple sclerosis [112], anorexia, bulimia ner-

Preprints (www.preprints.org) | NOT PEER-REVIEWED | Posted: 11 April 2022 doi:10.20944/preprints202204.0097.v1

vosa [113], Alzheimer's disease, Lewy body dementia, Parkinson's disease, and Huntington's disease [114]. Moreover, POP and DPP-IV have been associated with aggressive behaviors in normal and autistic adolescents [115].

Furthermore, peptidyl-dipeptidase ANCE (M02.003) is involved in the renin-angiotensin-aldosterone system (RAAS) that regulates blood pressure by hydrolyzing angiotensin I into angiotensin II (vasoconstrictor) and its physiological substrate bradykinin, which is a vasodilator [9]. Moreover, angiotensin-converting enzyme-2 (ACE-2, M02.006) is a regulator of heart function. Based on the ace2 gene knock-out experiments, disruption in mice causes severely impaired heart function whereas the disruption of ace2 homolog in Drosophila embryo resulted in a serious defect in the heart morphogenesis [116]. Besides, ACE2 is a functional receptor for SARS coronavirus [117] as shown in the crystal structure (PDB ID: 6M0J) of ACE2 bound to the SARS-CoV-2 spike with their receptor-binding domains [118].

On the other hand, neurolysin with PPC activity is widely distributed in the mammalian tissues and can be found in different subcellular locations, in cytosolic, membrane-bound forms, or with mitochondrial targeting sequences [119]. It is a neuropeptidase that cleaves short neuropeptides such as neurotensin, 13-residues neuropeptides that involve in the homeostasis of blood pressure, body temperature, gastrointestinal movement, and the release of brain hormones (dopamine, luteinizing hormone, and prolactin). Although there is no concrete evidence, neurolysin is hypothesized to be involved in the pathology of human diseases such as epilepsy, angiogenesis, tumor growth, sepsis, stroke, and metabolic disorder, together with thimet oligopeptidase (THOP1) and a POP [119].

3.3 Plants

The first plant PEP was isolated from carrot (*Daucus carota*) from the screening of over 40 vegetables and fruits, including spinach, carrot, pumpkin, soybean, green onion, and parsley for PEP activity [69]. Most of them showed low activity with spinach and carrot showing the highest PEP activity (1.11 unit/g and 0.81 unit/g, respectively). Carrot PEP was further analyzed since its extraction is easier while the enzyme activity of spinach was more varied. The enzyme was shown to be active at pH 7.3 and stable between pH 6-8.5. The enzyme showed activity towards Z-Gly-Pro-β-naphthylamide as the substrate, which is like PEP found in mammals and microbes. Further research showed that the enzyme purified from the carrot has more similarities to mammals than microbes [69]. Besides that, PEP extracted from spinach can recognize the scissile prolyl bond to cleave the 18 kDa protein of photosystem II, indicating a possible role in chloroplasts and photosynthesis [72].

POP genes (*CaPEP1*, *CaPEP2*, and *CaPEP3*) were found to be differentially expressed in two closely related *Coffea arabica* varieties, cultivars "Tall Mokka" and "Typica" [68]. These genes are responsible for the lateral shoot branching and branched phenotype. Besides, dipeptidyl-peptidase (DPP) II (S28.002) is shown to be involved in the protein mobilization during seed germination to provide nutrients for the growth of embryonic plants. A significant correlation between DPP-II activity, protein content, and free amino acid content during seed germination of *Vigna radiata* suggests that DPP-II breakdown protein storage in seed into free amino acid during the germination period [73].TsPAP1 gene encoding a prolyl aminopeptidase (S33.001) was upregulated in the shoots of triticale under harsh environments such as dry and salty conditions, as well as the presence of cadmium and aluminum ions in nutrient media [71]. Furthermore, the overexpression of TsPAP1 in transgenic *Arabidopsis thaliana* resulted in a faster flowering process and the production of more siliques [76]. These findings suggest that PPCEs play important roles in different plant growth and developmental stages.

Preprints (www.preprints.org) | NOT PEER-REVIEWED | Posted: 11 April 2022 doi:10.20944/preprints202204.0097.v1

On the other hand, omics studies have been conducted to discover digestive proteins that contribute to the botanical carnivory [120]. Enzymes in the pitcher fluids of *Nepenthes* species were found mainly comprising aspartic protease nepenthesins and neprosin [121,122], which suggests the importance of proteases in the adaptation and diversification of *Nepenthes* species. Furthermore, PPC activity has been shown in the native and recombinant neprosins to degrade gliadins from wheat [48,81].

4. Applications

4.1 Industrial applications

PPCEs have many uses in the industry. For example, PEP enzymes are useful for the gluten-free food processing industry for people with gluten intolerance, such as celiac disease. Celiac disease occurs in individuals with HLA-DQ2 or HLA-DQ8 genetic predisposition where the ingestion of gluten can trigger a T-cell immune response in the small intestine [123]. Gluten is a common protein that can be found in cereals, such as barley and wheat, which is proline-rich and resistant to digestion by pancreatic or gastric enzymes. High proteolytic resistance gluten peptides such as alpha-gliadin 33-mer and gamma-gliadin 26-mer peptides can bind to the HLA-DQ2 or HLA-DQ8 antigens. These peptides are presented to the pro-inflammatory T-cells, which can cause inflammation and damage to villi on the small intestine wall, leading to various complications [124]. The best treatment for celiac disease is a strict gluten-free diet to relieve symptoms, reversal of malabsorption, and restorative of villi. A study investigating five gluten-degrading enzyme supplements on the market showed that amylases, galactosidases, proteases, and/or subtilisin cannot eliminate the nine immunogenic epitopes of 26-mer and 33-mer [125]. In contrast, AN-PEP degrades all nine epitopes effectively at the pH range of the stomach at a much lower dose [7]. AN-PEP (S28.004) has been tested against three different types of wheat flours, *Triticum aestivum* (HD-2851, NIAW-917), *Triticum durum* (UAS-428), and *Triticum dicoccum* (DDK- 1025) for proteolytic degradation and shown to have 99.95% lesser gluten content than the control pasta. The sensory evaluation test showed that the quality of the treated wheat flour is comparable to the control pasta, despite having a brownish color [7]. This demonstrates the potential of PEP to be used in oral supplements for gluten degradation. Another study showed that the consumption of bread pre-digested with AN-PEP lowered the immunogenic gluten by approximately 40% [90]. Hence, AN-PEP pre-digestion is applicable in the bread production industry.

Furthermore, to test the efficiency of AN-PEP gluten degradation in a randomized placebo-controlled crossover study, 18 celiac disease patients were given a porridge containing 0.5 g gluten together with two tablets either containing a high or low dose of AN-PEP, or a placebo. In a meal physiological setting, samples were then taken from the stomach and duodenal content to calculate the gluten content. Results showed an over 50% reduction of gluten content in both stomach and duodenum as compared to placebo. Furthermore, gluten degradation was shown to be more apparent in the stomach compared to before it entered the duodenum, showing AN-PEP as a potent protease in degrading gluten content when provided in a meal setting [91].

Another study showed that AN-PEP degrades gluten in a dynamic system (TIM) that closely mimics the human gastrointestinal tract [94]. Gluten content measurements were taken from the stomach, duodenum, jejunum, and ileum compartments of individuals who ingest bread or standard fast-food processed in the TIM system with and without co-administration of AN-PEP. Based on the monoclonal antibody-based competition assays, Western blot analysis, and T-cell proliferation assays, most gluten was degraded in the stomach before it reaches the duodenum compartment. Hence, this experiment also showed that AN-PEP degrades gluten in a system that mimics human in-vivo digestion [94].

Preprints (www.preprints.org) | NOT PEER-REVIEWED | Posted: 11 April 2022 doi:10.20944/preprints202204.0097.v1

There are also efforts to utilize POP from *Sphingomonas capsulate* and *Myxococcus xanthus* as oral supplements for gluten degradation, but these proteases failed to detoxify gluten after irreversibly inactivated by pepsin and acidic pH in the stomach [95]. Instead, AN-PEP is more resistant to the acidic pH and pepsin in the stomach and has proven potent against gluten. However, reports also indicate that different types of meals need a different amount of AN-PEP for gluten detoxification. Acidic meals like carbonated drinks enhance AN-PEP activity while food proteins reduce the AN-PEP capacity for gluten detoxification, while not being affected by fats. Moreover, raw gluten is easier to be degraded by AN-PEP than baked gluten. Therefore, AN-PEP is not able to digest large portions of gluten, hence it should not be used to replace an entirely gluten-free diet, but rather to support digestion of low occasional gluten consumption [93]. Furthermore, the combination of native neprosin and nepenthesin proteins from *N.* × *ventrata* has also demonstrated the capability to digest gliadin [48].

On the other hand, PEP can reduce the hordein content in beer that may interact with polyphenol causing cloudy precipitation (chill-haze) during storage [98]. One alternative to removing the polyphenols that interact with the proline-rich residues is by removing the proline-rich proteins that are intolerant to gluten-sensitive individuals. Metallopeptidase M13 oligopeptidase O2 (M13.010) expressed in *Lactobacillus helveticus* WSU19 with PPC activity can effectively debitter aged Cheddar cheese. The oligopeptidase O2 was experimentally proven to cleave three sites after Pro196, Pro200, and Pro206 for the complete digestion of the bitter β-casein (f193-209) [126].

A study also showed that AN-PEP treated barley for five days during germination can reduce beer hordein content by 46% compared to control when tested using an R5 antibody-based competitive enzyme-linked immunosorbent assay [92]. In theory, a longer malting process will cause a higher cost, but the treatment of AN-PEP during the malting process does not affect the malting loss significantly [92]. Moreover, to improve the enzymatic activity of PEP, a study used immobilized proline-specific endoprotease (PSEP) or silica gel to prevent haze from forming inside the beer. Using the immobilized PSEP, it could retain up to 65% of its enzymatic activity as compared to the non-immobilized ones with better tolerance towards temperature and pH. Moreover, the enzyme can retain over 90% of its original activity even after six cycles. Hence, this provides an advantageous alternative for the beer brewing industry [98].

4.2 Therapeutic agents

Due to the important functions of certain PEP/POP in human cognitive diseases (described in 3.2), understanding the mechanism of PPCEs is useful for the design of drugs or enzyme inhibitors as therapeutics. PEP inhibitors can be categorized broadly into natural and synthetic inhibitors. Natural PEP inhibitors can be found in traditional medicinal herbs, such as isoquinoline alkaloid berberine from *Berberis vulgaris*, flavonoid baicalein from *Scutellaria baicalensis Georgi*, and alkaloid californidine from *Eschscholzia californica* [127]. Berberine and its derivatives were found to be effective for bipolar disorder and patented as PEP inhibitors in 2008 [128].

Aside from PEP, metallopeptidase M3 neurolysin (M03.002) with the ability to cleave multiple types of neuropeptides hinted at its potential as a single therapeutic target for multiple diseases. Hence, neurolysin and POP are currently being studied systematically as potential therapeutic targets to cure human brain diseases [129]. Moreover, metallopeptidase M2 such as peptidyl-dipeptidase ANCE (M02.003) and angiotensin-converting enzyme-2 (M02.006) are also therapeutic targets for human diseases. For instance, peptidyl-dipeptidase ANCE inhibitors were used in hypertension treatment [130]. Furthermore, a cell membrane chromatography study demonstrated that the third-generation antihistamine azelastine has an affinity toward ACE2 and provides antiviral properties by inhibiting the entry of pseudovirus *in vitro* [131]. Hence, azelastine could be a potential

Preprints (www.preprints.org) | NOT PEER-REVIEWED | Posted: 11 April 2022 doi:10.20944/preprints202204.0097.v1

candidate for drug repurposing in COVID-19 treatment. Other than human PPCE, rational drug designs that target POP of *Trypanosoma brucei* and *T. cruzi* are currently in progress to combat Chagas diseases and human African trypanosomiasis [132].

4.3 Proteomics tool

PEP has a unique prolyl cleaving proteolytic mechanism compared to other protein cleaving families such as trypsin, which is usually preferred in mass spectrometry (MS) - based proteomics [133]. Besides trypsin, the activity of AN-PEP for mass spectrometry is also comparable to that conventionally used enzyme pepsin. The number of peptides generated by AN-PEP at a lower concentration is equivalent to pepsin [134]. Moreover, the peptides generated are shorter than peptides generated by pepsin allowing better insight with higher resolution [134]. Hence, the authors recommend the use of pepsin digestion complemented with AN-PEP for a better resolution in MS studies.

Neprosin with PPC activity was applied in the analysis of histone modifications using the proteomics method due to its selective prolyl endoprotease nature as compared to the conventional trypsin-based methods to study the information of the histones H3 and H4 [105]. For example, neprosin from *Nepenthes* × *ventrata* was used to digest 1,251 HeLa cell proteins for a proteomics study [81], which showed that almost half of the result gives unique peptides compared to trypsin, thus allowing detailed analysis of protein post-translational modifications.

5. Protein engineering

Studies to improve the activity of the PEP enzymes have been performed through protein engineering. For example, PEP mutagenesis on residues F263A and E184G on the β-propeller domain of the novel *Stenotrophomonas maltophilia* prolyl endopeptidase (SmPEP) improves the enzymatic activity of the enzymes towards synthetic peptides. The introduction of mutants on these specific residues weakens the inter-domain interaction of the enzymes to reduce the restriction of bigger substrates to enter the active site [54]. The increased specificity of the enzyme activity was recorded when random and site-directed saturation mutagenesis was performed on prolyl aminopeptidase derived from *Aspergillus oryzae* [100]. Mutagenesis at C185V allowed a higher resistance towards high temperature, broader acidity range, and longer half-life compared to wild type making it a good candidate for many industrial sectors [100].

Moreover, site-directed mutagenesis of POP from *Flavobacterium meningosepticum* (Fm-POP) that was expressed in the wheat endosperm showed the ability to reduce gluten content under gastrointestinal conditions with a higher ability to tolerate high temperatures over 37°C up to 90°C [51]. Gluten peptides can be digested up to 67% using Fm-POP in combination with barley endoprotease B2 (EP-HvB2) [101]. Hence, the modifications of these enzymes allow them to function under harsh conditions without affecting their enzyme efficiencies.

6. Conclusion

This review explores the structure-function studies of PPCEs from different taxa and highlights many of their biological functions. PPCEs found in diverse organisms are useful in various ways given their unique capability to degrade proline-rich proteins. Moreover, enzyme characterization studies for both the native and recombinant PPCEs from various species suggest a promising potential for PPCEs to be applied according to their optimum conditions for various purposes. This review provides examples of extensive

PPCE applications in the beer-brewing industry, as potential therapeutic agents for individuals intolerant to gluten, as well as applications in proteomics analysis. Hopefully, further protein engineering and structure-function studies with the aid of *ab initio* structural prediction will uncover more useful PPCEs for new applications.

Author Contributions: AB and TTT wrote the manuscript. HHG reviewed and edited the manuscript.

Funding: The research group was supported by the Malaysian Ministry of Higher Education Fundamental Research Grant Scheme (FRGS/1/2019/STG05/UKM/02/10) and Universiti Kebangsaan Malaysia Research University Grant (DIP-2020-005).

Data Availability Statement: "Not applicable"

Acknowledgments: We thank the funding agency for supporting the research from our group.

Conflicts of Interest: The authors declare that the research was conducted in the absence of any commercial or financial relationships that could be construed as a potential conflict of interest.

References

1. Rawlings, N.D.; Barrett, A.J.; Thomas, P.D.; Huang, X.; Bateman, A.; Finn, R.D. The MEROPS database of proteolytic enzymes, their substrates and inhibitors in 2017 and a comparison with peptidases in the PANTHER database. *Nucleic Acids Res.* **2018**, *46*, 624-632
2. Rawlings, N.D.; Barrett, A.J.; Bateman, A. Asparagine peptide lyases: a seventh catalytic type of proteolytic enzymes. *J Biol Chem* **2011**, *286*, 38321-38328
3. Rawlings, N.D.; Bateman, A. Origins of peptidases. *Biochimie* **2019**, *166*, 4-18
4. Hedstrom, L. Serine protease mechanism and specificity. *Chem Rev* **2002**, *102*, 4501-4524
5. Gass, J.; Khosla, C. Prolyl endopeptidases. *Cell Mol Life Sci* **2007**, *64*, 345-355
6. Darkoh, C.; El-Bouhssini, M.; Baum, M.; Clack, B. Characterization of a prolyl endoprotease from *Eurygaster integriceps* Puton (Sunn pest) infested wheat. *Arch Insect Biochem Physiol* **2010**, *74*, 163-178
7. Mohan Kumar, B.V.; Sarabhai, S.; Prabhasankar, P. Targeted degradation of gluten proteins in wheat flour by prolyl endoprotease and its utilization in low immunogenic pasta for gluten sensitivity population. *J. Cereal Sci.* **2019**, *87*, 59-67
8. Mann, K.S.; Chisholm, J.; Sanfaçon, H. Strawberry mottle virus (Family Secoviridae, Order Picornavirales) encodes a novel glutamic protease to process the RNA2 Polyprotein at two cleavage sites. *J Virol* **2019**, *93*,
9. Wijffels, G.; Fitzgerald, C.; Gough, J.; Riding, G.; Elvin, C.; Kemp, D.; Willadsen, P. Cloning and characterisation of angiotensin-converting enzyme from the dipteran species, *Haematobia irritans exigua*, and its expression in the maturing male reproductive system. *Eur J Biochem* **1996**, *237*, 414-423
10. Vickers, C.; Hales, P.; Kaushik, V.; Dick, L.; Gavin, J.; Tang, J.; Godbout, K.; Parsons, T.; Baronas, E.; Hsieh, F.; et al. Hydrolysis of biological peptides by human angiotensin-converting enzyme-related carboxypeptidase. *J Biol Chem* **2002**, *277*, 14838-14843
11. Barrett, A.J.; Dando, P.M. Neurolysin. In *Handbook of proteolytic enzymes: Second edition*; 2004; Volume 1, pp. 356-360.
12. Maruyama, S. Peptidyl-dipeptidase (*Streptomyces*). In *Handbook of proteolytic enzymes: Second edition*; 2004; Volume 1, pp. 1030-1031.
13. Trummal, K.; Vija, H.; Subbi, J.; Siigur, J. MALDI-TOF mass spectrometry analysis of substrate specificity of lebetase, a direct-acting fibrinolytic metalloproteinase from *Vipera lebetina* snake venom. *Biochim Biophys Acta* **2000**, *1476*, 331-336
14. Akao, P.K.; Tonoli, C.C.; Navarro, M.S.; Cintra, A.C.; Neto, J.R.; Arni, R.K.; Murakami, M.T. Structural studies of BmooMPalpha-I, a non-hemorrhagic metalloproteinase from *Bothrops moojeni* venom. *Toxicon* **2010**, *55*, 361-368
15. Soeryapranata, E.; Powers, J.R.; Ünlü, G. Cloning and characterization of debittering peptidases, PepE, PepO, PepO2, PepO3, and PepN, of *Lactobacillus helveticus* WSU19. *Int. Dairy J.* **2007**, *17*, 1096-1106

16. Chen, Y.S.; Christensen, J.E.; Broadbent, J.R.; Steele, J.L. Identification and characterization of *Lactobacillus helveticus* PepO2, an endopeptidase with post-proline specificity. *Appl Environ Microbiol* **2003**, *69*, 1276-1282
17. Hensbergen, P.J.; Klychnikov, O.I.; Bakker, D.; van Winden, V.J.; Ras, N.; Kemp, A.C.; Cordfunke, R.A.; Dragan, I.; Deelder, A.M.; Kuijper, E.J.; et al. A novel secreted metalloprotease (CD2830) from *Clostridium difficile* cleaves specific proline sequences in LPXTG cell surface proteins. *Mol Cell Proteomics* **2014**, *13*, 1231-1244
18. Klychnikov, O.I.; Shamorkina, T.M.; Weeks, S.D.; van Leeuwen, H.C.; Corver, J.; Drijfhout, J.W.; van Veelen, P.A.; Sluchanko, N.N.; Strelkov, S.V.; Hensbergen, P.J. Discovery of a new Pro-Pro endopeptidase, PPEP-2, provides mechanistic insights into the differences in substrate specificity within the PPEP family. *J Biol Chem* **2018**, *293*, 11154-11165
19. Fujiyama, Y.; Iwaki, M.; Hodohara, K.; Hosoda, S.; Kobayashi, K. The site of cleavage in human alpha chains of IgA1 and IgA2:A2m(1) allotype paraproteins by the clostridial IGA protease. *Mol Immunol* **1986**, *23*, 147-150
20. Waack, U.; Warnock, M.; Yee, A.; Huttinger, Z.; Smith, S.; Kumar, A.; Deroux, A.; Ginsburg, D.; Mobley, H.L.T.; Lawrence, D.A.; et al. CpaA Is a glycan-specific adamalysin-like protease secreted by *Acinetobacter baumannii* that inactivates coagulation factor XII. *mBio* **2018**, *9*,
21. Poulsen, K.; Kilian, M. IgA1-specific serine endopeptidase. In *Handbook of Proteolytic Enzymes*; 2013; Volume 3, pp. 3088-3092.
22. Mistry, D.V.; Stockley, R.A. The cleavage specificity of an IgA1 protease from *Haemophilus influenzae*. *Virulence* **2011**, *2*, 103-110
23. Shan, L.; Marti, T.; Sollid, L.M.; Gray, G.M.; Khosla, C. Comparative biochemical analysis of three bacterial prolyl endopeptidases: implications for coeliac sprue. *The Biochemical journal* **2004**, *383*, 311-318
24. Harris, M.N.; Madura, J.D.; Ming, L.J.; Harwood, V.J. Kinetic and mechanistic studies of prolyl oligopeptidase from the hyperthermophile *Pyrococcus furiosus*. *J Biol Chem* **2001**, *276*, 19310-19317
25. Lambeir, A.M.; Proost, P.; Durinx, C.; Bal, G.; Senten, K.; Augustyns, K.; Scharpé, S.; Van Damme, J.; De Meester, I. Kinetic investigation of chemokine truncation by CD26/dipeptidyl peptidase IV reveals a striking selectivity within the chemokine family. *J Biol Chem* **2001**, *276*, 29839-29845
26. Misumi, Y.; Ikehara, Y. Dipeptidyl-peptidases A and B. In *Handbook of Proteolytic Enzymes*; 2013; Volume 3, pp. 3390-3391.
27. Lee, K.N.; Jackson, K.W.; Christiansen, V.J.; Lee, C.S.; Chun, J.G.; McKee, P.A. Antiplasmin-cleaving enzyme is a soluble form of fibroblast activation protein. *Blood* **2006**, *107*, 1397-1404
28. Monod, M.; Beauvais, A. Dipeptidyl-peptidases IV and V of *Aspergillus*. In *Handbook of Proteolytic Enzymes*; 2013; Volume 3, pp. 3392-3394.
29. Nakajima, Y.; Ito, K.; Toshima, T.; Egawa, T.; Zheng, H.; Oyama, H.; Wu, Y.F.; Takahashi, E.; Kyono, K.; Yoshimoto, T. Dipeptidyl aminopeptidase IV from *Stenotrophomonas maltophilia* exhibits activity against a substrate containing a 4-hydroxyproline residue. *J Bacteriol* **2008**, *190*, 7819-7829
30. Banbula, A.; Bugno, M.; Goldstein, J.; Yen, J.; Nelson, D.; Travis, J.; Potempa, J. Emerging family of proline-specific peptidases of *Porphyromonas gingivalis*: purification and characterization of serine dipeptidyl peptidase, a structural and functional homologue of mammalian prolyl dipeptidyl peptidase IV. *Infect Immun* **2000**, *68*, 1176-1182
31. Banbula, A.; Mak, P.; Bugno, M.; Silberring, J.; Dubin, A.; Nelson, D.; Travis, J.; Potempa, J. Prolyl tripeptidyl peptidase from *Porphyromonas gingivalis*. A novel enzyme with possible pathological implications for the development of periodontitis. *J Biol Chem* **1999**, *274*, 9246-9252
32. Ajami, K.; Pitman, M.R.; Wilson, C.H.; Park, J.; Menz, R.I.; Starr, A.E.; Cox, J.H.; Abbott, C.A.; Overall, C.M.; Gorrell, M.D. Stromal cell-derived factors 1alpha and 1beta, inflammatory protein-10 and interferon-inducible T cell chemo-attractant are novel substrates of dipeptidyl peptidase 8. *FEBS Lett* **2008**, *582*, 819-825
33. Geiss-Friedlander, R.; Parmentier, N.; Möller, U.; Urlaub, H.; Van den Eynde, B.J.; Melchior, F. The cytoplasmic peptidase DPP9 is rate-limiting for degradation of proline-containing peptides. *J Biol Chem* **2009**, *284*, 27211-27219

34. Grellier, P.; Vendeville, S.; Joyeau, R.; Bastos, I.M.; Drobecq, H.; Frappier, F.; Teixeira, A.R.; Schrével, J.; Davioud-Charvet, E.; Sergheraert, C.; et al. Trypanosoma cruzi prolyl oligopeptidase Tc80 is involved in nonphagocytic mammalian cell invasion by trypomastigotes. *J Biol Chem* **2001**, *276*, 47078-47086
35. Portugal, B.; Motta, F.N.; Correa, A.F.; Nolasco, D.O.; de Almeida, H.; Magalhães, K.G.; Atta, A.L.; Vieira, F.D.; Bastos, I.M.; Santana, J.M. *Mycobacterium tuberculosis* prolyl oligopeptidase induces *in vitro* secretion of proinflammatory cytokines by peritoneal macrophages. *Front Microbiol* **2017**, *8*, 155
36. Hatanaka, T.; Yamasato, A.; Arima, J.; Usuki, H.; Yamamoto, Y.; Kumagai, Y. Extracellular production and characterization of *Streptomyces* X-prolyl dipeptidyl aminopeptidase. *Appl Biochem Biotechnol* **2011**, *164*, 475-486
37. Shan, L.; Mathews, II; Khosla, C. Structural and mechanistic analysis of two prolyl endopeptidases: role of interdomain dynamics in catalysis and specificity. *Proc Natl Acad Sci U S A* **2005**, *102*, 3599-3604
38. Luo, H.; Hong, S.-Y.; Sgambelluri, R.M.; Angelos, E.; Li, X.; Walton, J.D. Peptide macrocyclization catalyzed by a prolyl oligopeptidase involved in α-amanitin biosynthesis. *Chem Biol* **2014**, *21*, 1610-1617
39. Yamamoto, F.; Morisaka, H.; Ueda, M.; Watanabe, K. Molecular characterization of a prolyl endopeptidase from a feather-degrading thermophile *Meiothermus ruber* H328. *J Biochem* **2020**, *168*, 499-508
40. Jobin, M.C.; Martinez, G.; Motard, J.; Gottschalk, M.; Grenier, D. Cloning, purification, and enzymatic properties of dipeptidyl peptidase IV from the swine pathogen *Streptococcus suis*. *J Bacteriol* **2005**, *187*, 795-799
41. Zhao, X.; Southwick, K.; Cardasis, H.L.; Du, Y.; Lassman, M.E.; Xie, D.; El-Sherbeini, M.; Geissler, W.M.; Pryor, K.D.; Verras, A.; et al. Peptidomic profiling of human cerebrospinal fluid identifies YPRPIHPA as a novel substrate for prolylcarboxypeptidase. *Proteomics* **2010**, *10*, 2882-2886
42. Miyazono, K.-i.; Kubota, K.; Takahashi, K.; Tanokura, M. Crystal structure and substrate recognition mechanism of the prolyl endoprotease PEP from *Aspergillus niger*. *Biochem. Biophys. Res. Commun.* **2022**, *591*, 76-81
43. Ito, K.; Nakajima, Y.; Yoshimoto, T. Prolyl aminopeptidase. In *Handbook of proteolytic enzymes*; 2013; Volume 3, pp. 3438-3443.
44. Huang, Y.; Tanaka, T. Characterization of two putative prolinases (PepR1 and PepR2) from *Lactobacillus plantarum* WCFS1: occurrence of two isozymes with structural similarity and different catalytic properties. *Biochim Biophys Acta* **2015**, *1854*, 91-100
45. Stepaniak, L. Isolation and characterization of proline iminopeptidase from *Propionibacterium freudenreichii* ATCC 9614. *Nahrung* **2000**, *44*, 102-106
46. Umezawa, Y.; Yokoyama, K.; Kikuchi, Y.; Date, M.; Ito, K.; Yoshimoto, T.; Matsui, H. Novel prolyl tri/tetra-peptidyl aminopeptidase from *Streptomyces mobaraensis*: substrate specificity and enzyme gene cloning. *J Biochem* **2004**, *136*, 293-300
47. Kuwabara, T. Characterization of a prolyl endopeptidase from spinach thylakoids. *FEBS Lett* **1992**, *300*, 127-130
48. Rey, M.; Yang, M.; Lee, L.; Zhang, Y.; Sheff, J.G.; Sensen, C.W.; Mrazek, H.; Halada, P.; Man, P.; McCarville, J.L.; et al. Addressing proteolytic efficiency in enzymatic degradation therapy for celiac disease. *Sci Rep* **2016**, *6*, 30980
49. Ellis-Guardiola, K.; Rui, H.; Beckner, R.L.; Srivastava, P.; Sukumar, N.; Roux, B.; Lewis, J.C. Crystal structure and conformational dynamics of *Pyrococcus furiosus* prolyl oligopeptidase. *Biochemistry* **2019**, *58*, 1616-1626
50. Li, M.; Chen, C.; Davies, D.R.; Chiu, T.K. Induced-fit mechanism for prolyl endopeptidase. *J Biol Chem* **2010**, *285*, 21487-21495
51. Osorio, C.E.; Wen, N.; Mejias, J.H.; Liu, B.; Reinbothe, S.; von Wettstein, D.; Rustgi, S. Development of wheat genotypes expressing a glutamine-specific endoprotease from barley and a prolyl endopeptidase from *Flavobacterium meningosepticum* or *Pyrococcus furiosus* as a potential remedy to celiac disease. *Funct Integr Genomics* **2019**, *19*, 123-136
52. Schulze, A.; Wermann, M.; Demuth, H.U.; Yoshimoto, T.; Ramsbeck, D.; Schlenzig, D.; Schilling, S. Continuous assays for meprin alpha and beta using prolyl tripeptidyl aminopeptidase (PtP) from *Porphyromonas gingivalis*. *Anal Biochem* **2018**, *559*, 11-16
53. Yoshimoto, T.; Kabashima, T.; Uchikawa, K.; Inoue, T.; Tanaka, N.; Nakamura, K.T.; Tsuru, M.; Ito, K. Crystal structure of prolyl aminopeptidase from *Serratia marcescens*. *J Biochem* **1999**, *126*, 559-565

54. Yu, J.; Wu, J.; Xie, D.; Du, L.; Tang, Y.J.; Xie, J.; Wei, D. Characterization and rational design for substrate specificity of a prolyl endopeptidase from *Stenotrophomonas maltophilia*. *Enzyme Microb Technol* **2020**, *138*, 109548
55. Kang, C.; Yu, X.W.; Xu, Y. Cloning and expression of a novel prolyl endopeptidase from *Aspergillus oryzae* and its application in beer stabilization. *J Ind Microbiol Biotechnol* **2015**, *42*, 263-272
56. Bastos, I.M.D.; Motta, F.N.; Grellier, P.; Santana, J.M. Parasite prolyl oligopeptidases and the challenge of designing chemotherapeuticals for Chagas disease, leishmaniasis and African trypanosomiasis. *Current medicinal chemistry* **2013**, *20*, 3103-3115
57. Bastos, I.M.; Grellier, P.; Martins, N.F.; Cadavid-Restrepo, G.; de Souza-Ault, M.R.; Augustyns, K.; Teixeira, A.R.; Schrével, J.; Maigret, B.; da Silveira, J.F.; et al. Molecular, functional and structural properties of the prolyl oligopeptidase of *Trypanosoma cruzi* (POP Tc80), which is required for parasite entry into mammalian cells. *Biochem J* **2005**, *388*, 29-38
58. Houard, X.; Williams, T.A.; Michaud, A.; Dani, P.; Isaac, R.E.; Shirras, A.D.; Coates, D.; Corvol, P. The *Drosophila melanogaster*-related angiotensin-I-converting enzymes Acer and Ance--distinct enzymic characteristics and alternative expression during pupal development. *Eur J Biochem* **1998**, *257*, 599-606
59. Li, W.Y.; Li, Y.; Chen, Y.L.; Hu, J.J.; Mengist, H.M.; Liu, G.M.; Jin, T.; Cao, M.J. Characterization and crystal structure of prolyl endopeptidase from abalone (*Haliotis discus hannai*). *Food Chem* **2020**, *333*, 127452
60. Goossens, F.; De Meester, I.; Vanhoof, G.; Hendriks, D.; Vriend, G.; Scharpé, S. The purification, characterization and analysis of primary and secondary-structure of prolyl oligopeptidase from human lymphocytes. Evidence that the enzyme belongs to the alpha/beta hydrolase fold family. *Eur J Biochem* **1995**, *233*, 432-441
61. Myöhänen, T.T.; Pyykkö, E.; Männistö, P.T.; Carpen, O. Distribution of prolyl oligopeptidase in human peripheral tissues and in ovarian and colorectal tumors. *J Histochem Cytochem* **2012**, *60*, 706-715
62. Hiramatsu, H.; Kyono, K.; Higashiyama, Y.; Fukushima, C.; Shima, H.; Sugiyama, S.; Inaka, K.; Yamamoto, A.; Shimizu, R. The structure and function of human dipeptidyl peptidase IV, possessing a unique eight-bladed beta-propeller fold. *Biochem Biophys Res Commun* **2003**, *302*, 849-854
63. Soisson, S.M.; Patel, S.B.; Abeywickrema, P.D.; Byrne, N.J.; Diehl, R.E.; Hall, D.L.; Ford, R.E.; Reid, J.C.; Rickert, K.W.; Shipman, J.M.; et al. Structural definition and substrate specificity of the S28 protease family: the crystal structure of human prolylcarboxypeptidase. *BMC Struct Biol* **2010**, *10*, 16-16
64. Towler, P.; Staker, B.; Prasad, S.G.; Menon, S.; Tang, J.; Parsons, T.; Ryan, D.; Fisher, M.; Williams, D.; Dales, N.A.; et al. ACE2 X-ray structures reveal a large hinge-bending motion important for inhibitor binding and catalysis. *J Biol Chem* **2004**, *279*, 17996-18007
65. Brown, C.K.; Madauss, K.; Lian, W.; Beck, M.R.; Tolbert, W.D.; Rodgers, D.W. Structure of neurolysin reveals a deep channel that limits substrate access. *Proc Natl Acad Sci U S A* **2001**, *98*, 3127-3132
66. Myöhänen, T.T.; Venäläinen, J.I.; García-Horsman, J.A.; Piltonen, M.; Männistö, P.T. Distribution of prolyl oligopeptidase in the mouse whole-body sections and peripheral tissues. *Histochem Cell Biol* **2008**, *130*, 993-1003
67. Fülöp, V.; Böcskei, Z.; Polgár, L. Prolyl oligopeptidase: an unusual beta-propeller domain regulates proteolysis. *Cell* **1998**, *94*, 161-170
68. Singh, R.K.; Irikura, B.; Nagai, C.; Albert, H.H.; Kumagai, M.H.; Paull, R.E.; Moore, P.H.; Wang, M.-l.J.T.P.B. Characterization of prolyl oligopeptidase genes differentially expressed between two cultivars of *Coffea arabica* L. *Trop. Plant Biol.* **2011**, *4*, 203-216
69. Yoshimoto, T.; Abdus Sattar, A.K.M.; Hirose, W.; Tsuru, D. Studies on prolyl endopeptidase from carrot (*Daucus carota*): purification and enzymatic properties. *Biochim Biophys Acta Proteins Proteom* **1987**, *916*, 29-37
70. Ravee, R.; Baharin, A.; Cho, W.T.; Ting, T.Y.; Goh, H.H. Protease activity is maintained in *Nepenthes ampullaria* digestive fluids depleted of endogenous proteins with compositional changes. *Physiol Plant* **2021**, *173*, 1967-1978
71. Szawłowska, U.; Grabowska, A.; Zdunek-Zastocka, E.; Bielawski, W. TsPAP1 encodes a novel plant prolyl aminopeptidase whose expression is induced in response to suboptimal growth conditions. *Biochem Biophys Res Commun* **2012**, *419*, 104-109

72. Kuwabara, T.; Suzuki, K. A prolyl endoproteinase that acts specifically on the extrinsic 18-kDa protein of photosystem II: purification and further characterization. *Plant Cell Physiol* **1994**, *35*, 665-675
73. Khaket, T.P.; Dhanda, S.; Jodha, D.; Singh, J. Purification and biochemical characterization of dipeptidyl peptidase-II (DPP7) homologue from germinated *Vigna radiata* seeds. *Bioorg Chem* **2015**, *63*, 132-141
74. Tarragó, T.; Martín-Benito, J.; Sabidó, E.; Claasen, B.; Madurga, S.; Gairí, M.; Valpuesta, J.M.; Giralt, E. A new side opening on prolyl oligopeptidase revealed by electron microscopy. *FEBS Lett* **2009**, *583*, 3344-3348
75. Kaushik, S.; Sowdhamini, R. Structural analysis of prolyl oligopeptidases using molecular docking and dynamics: insights into conformational changes and ligand binding. *PLoS One* **2011**, *6*, e26251
76. Zdunek-Zastocka, E.; Grabowska, A.; Branicki, T.; Michniewska, B. Biochemical characterization of the triticale TsPAP1, a new type of plant prolyl aminopeptidase, and its impact on proline content and flowering time in transgenic *Arabidopsis* plants. *Plant Physiol Biochem* **2017**, *116*, 18-26
77. Shan, L.; Marti, T.; Sollid, L.M.; Gray, G.M.; Khosla, C. Comparative biochemical analysis of three bacterial prolyl endopeptidases: implications for coeliac sprue. *Biochem J* **2004**, *383*, 311-318
78. Miyazono, K.I.; Kubota, K.; Takahashi, K.; Tanokura, M. Crystal structure and substrate recognition mechanism of the prolyl endoprotease PEP from *Aspergillus niger*. *Biochem Biophys Res Commun* **2022**, *591*, 76-81
79. Marinova, M.; Dolashki, A.; Altenberend, F.; Stevanovic, S.; Voelter, W.; Tchorbanov, B. Characterization of an aminopeptidase and a proline iminopeptidase from cabbage leaves. *Z Naturforsch C J Biosci* **2008**, *63*, 105-112
80. Ting, T.Y.; Baharin, A.; Ramzi, A.B.; Ng, C.-L.; Goh, H.-H. Neprosin belongs to a new family of glutamic peptidase based on *in silico* evidence. **2022**, *bioRxiv* DOI: 10.1101/2022.02.22.481544
81. Schräder, C.U.; Lee, L.; Rey, M.; Sarpe, V.; Man, P.; Sharma, S.; Zabrouskov, V.; Larsen, B.; Schriemer, D.C. Neprosin, a selective prolyl endoprotease for bottom-up proteomics and histone mapping. *Mol Cell Proteomics* **2017**, *16*, 1162-1171
82. Kim, H.M.; Shin, D.R.; Yoo, O.J.; Lee, H.; Lee, J.O. Crystal structure of *Drosophila* angiotensin I-converting enzyme bound to captopril and lisinopril. *FEBS Lett* **2003**, *538*, 65-70
83. Schacherl, M.; Pichlo, C.; Neundorf, I.; Baumann, U. Structural basis of proline-proline peptide bond specificity of the metalloprotease Zmp1 implicated in motility of *Clostridium difficile*. *Structure* **2015**, *23*, 1632-1642
84. Ekici, O.D.; Paetzel, M.; Dalbey, R.E. Unconventional serine proteases: variations on the catalytic Ser/His/Asp triad configuration. *Protein Sci.* **2008**, *17*, 2023-2037
85. Inoue, T.; Ito, K.; Tozaka, T.; Hatakeyama, S.; Tanaka, N.; Nakamura, K.T.; Yoshimoto, T. Novel inhibitor for prolyl aminopeptidase from *Serratia marcescens* and studies on the mechanism of substrate recognition of the enzyme using the inhibitor. *Arch Biochem Biophys* **2003**, *416*, 147-154
86. Ito, K.; Inoue, T.; Kabashima, T.; Kanada, N.; Huang, H.S.; Ma, X.; Azmi, N.; Azab, E.; Yoshimoto, T. Substrate recognition mechanism of prolyl aminopeptidase from *Serratia marcescens*. *J Biochem* **2000**, *128*, 673-678
87. Nakajima, Y.; Ito, K.; Sakata, M.; Xu, Y.; Nakashima, K.; Matsubara, F.; Hatakeyama, S.; Yoshimoto, T. Unusual extra space at the active site and high activity for acetylated hydroxyproline of prolyl aminopeptidase from *Serratia marcescens*. *J Bacteriol* **2006**, *188*, 1599-1606
88. Pillai, B.; Cherney, M.M.; Hiraga, K.; Takada, K.; Oda, K.; James, M.N. Crystal structure of scytalidoglutamic peptidase with its first potent inhibitor provides insights into substrate specificity and catalysis. *J Mol Biol* **2007**, *365*, 343-361
89. Kang, C.; Yu, X.; Xu, Y.J.J.o.M.C.B.-e. A codon-optimized endoprotease Endo-Pro-*Aspergillus niger*: Over expression and high-density fermentation in *Pichia pastoris*. *J. Mol. Catal. B Enzym.* **2014**, *104*, 64-69
90. Rees, D.; Holtrop, G.; Chope, G.; Moar, K.M.; Cruickshank, M.; Hoggard, N. A randomised, double-blind, cross-over trial to evaluate bread, in which gluten has been pre-digested by prolyl endoprotease treatment, in subjects self-reporting benefits of adopting a gluten-free or low-gluten diet. *Br J Nutr* **2018**, *119*, 496-506
91. König, J.; Holster, S.; Bruins, M.J.; Brummer, R.J. Randomized clinical trial: Effective gluten degradation by *Aspergillus niger*-derived enzyme in a complex meal setting. *Sci. Rep.* **2017**, *7*, 13100

92. Taylor, J.P.; Jacob, F.; Zannini, E.; Arendt, E.K. Reduction of hordein content in beer by applying prolyl endoprotease to the malting process. *J Am Soc Brew Chem* **2017**, *75*, 262-268
93. Montserrat, V.; Bruins, M.J.; Edens, L.; Koning, F. Influence of dietary components on *Aspergillus niger* prolyl endoprotease mediated gluten degradation. *Food Chem* **2015**, *174*, 440-445
94. Mitea, C.; Havenaar, R.; Drijfhout, J.W.; Edens, L.; Dekking, L.; Koning, F. Efficient degradation of gluten by a prolyl endoprotease in a gastrointestinal model: implications for coeliac disease. *Gut* **2008**, *57*, 25-32
95. Stepniak, D.; Spaenij-Dekking, L.; Mitea, C.; Moester, M.; de Ru, A.; Baak-Pablo, R.; van Veelen, P.; Edens, L.; Koning, F. Highly efficient gluten degradation with a newly identified prolyl endoprotease: implications for celiac disease. *Am J Physiol Gastrointest Liver Physiol* **2006**, *291*, G621-629
96. Sebela, M.; Rehulka, P.; Kábrt, J.; Rehulková, H.; Ozdian, T.; Raus, M.; Franc, V.; Chmelík, J. Identification of N-glycosylation in prolyl endoprotease from *Aspergillus niger* and evaluation of the enzyme for its possible application in proteomics. *J Mass Spectrom* **2009**, *44*, 1587-1595
97. Lopez, M.; Edens, L. Effective prevention of chill-haze in beer using an acid proline-specific endoprotease from *Aspergillus niger*. *J. Agric. Food Chem.* **2005**, *53*, 7944-7949
98. Zhao, F.; Hou, T.; Wang, J.; Jiang, Y.; Huang, S.; Wang, Q.; Xian, M.; Mu, X. Immobilization of proline-specific endoprotease on nonporous silica nanoparticles functionalized with amino group. *Bioproc Biosyst Eng* **2017**, *40*, 1-7
99. Kang, C.; Yu, X.W.; Xu, Y. Gene cloning and enzymatic characterization of an endoprotease Endo-Pro-*Aspergillus niger*. *J Ind Microbiol Biotechnol* **2013**, *40*, 855-864
100. Liu, D.; Zhang, D.; Huang, Q.; Gu, L.; Zhou, N.; Tian, Y. Mutagenesis for improvement of activity and stability of prolyl aminopeptidase from *Aspergillus oryzae*. *Appl Biochem Biotechnol* **2020**, *191*, 1483-1498
101. Osorio, C.E.; Wen, N.; Mejías, J.H.; Mitchell, S.; von Wettstein, D.; Rustgi, S. Directed-mutagenesis of *Flavobacterium meningosepticum* prolyl-oligopeptidase and a glutamine-specific endopeptidase from barley. *Front. Nutr.* **2020**, *7*, 11
102. Shetty, R.; Vestergaard, M.; Jessen, F.; Hägglund, P.; Knorr, V.; Koehler, P.; Prakash, H.S.; Hobley, T.J. Discovery, cloning and characterisation of proline specific prolyl endopeptidase, a gluten degrading thermo-stable enzyme from *Sphaerobacter thermophiles*. *Enzyme Microb Technol* **2017**, *107*, 57-63
103. Yandamuri, R.C.; Gautam, R.; Darkoh, C.; Dareddy, V.; El-Bouhssini, M.; Clack, B.A. Cloning, expression, sequence analysis and homology modeling of the prolyl endoprotease from *Eurygaster integriceps Puton*. *Insects* **2014**, *5*, 762-782
104. Venäläinen, J.I.; Juvonen, R.O.; Forsberg, M.M.; Garcia-Horsman, A.; Poso, A.; Wallen, E.A.; Gynther, J.; Männistö, P.T. Substrate-dependent, non-hyperbolic kinetics of pig brain prolyl oligopeptidase and its tight binding inhibition by JTP-4819. *Biochem Pharmacol* **2002**, *64*, 463-471
105. Schräder, C.U.; Ziemianowicz, D.S.; Merx, K.; Schriemer, D.C. Simultaneous proteoform analysis of histones H3 and H4 with a simplified middle-down proteomics method. *Anal. Chem.* **2018**, *90*, 3083-3090
106. Salamin, K.; Eugster, P.J.; Jousson, O.; Waridel, P.; Grouzmann, E.; Monod, M. AoS28D, a proline-Xaa carboxypeptidase secreted by *Aspergillus oryzae*. *Appl Microbiol Biotechnol* **2017**, *101*, 4129-4137
107. Myöhänen, T.T.; Venäläinen, J.I.; Tupala, E.; Garcia-Horsman, J.A.; Miettinen, R.; Männistö, P.T. Distribution of immunoreactive prolyl oligopeptidase in human and rat brain. *Neurochem Res* **2007**, *32*, 1365-1374
108. Kushnareva, E.Y.; Krupina, N.A.; Khlebnikova, N.N.; Zolotov, N.N.; Kryzhanovskii, G.N. Activities of proline-specific peptidases in brain structures of rats with experimental anxiety-depressive state caused by administration of dipeptidyl peptidase IV inhibitor in the early postnatal period. *Bull Exp Biol Med* **2011**, *151*, 675-679
109. Triposkiadis, F.; Xanthopoulos, A.; Starling, R.C.; Iliodromitis, E. Obesity, inflammation, and heart failure: links and misconceptions. *Heart Fail Rev* **2021**,
110. Maes, M. Evidence for an immune response in major depression: a review and hypothesis. *Prog Neuropsychopharmacol Biol Psychiatry* **1995**, *19*, 11-38

111. Maes, M.; Goossens, F.; Scharpé, S.; Meltzer, H.Y.; D'Hondt, P.; Cosyns, P. Lower serum prolyl endopeptidase enzyme activity in major depression: further evidence that peptidases play a role in the pathophysiology of depression. *Biol Psychiatry* **1994**, *35*, 545-552

112. Tenorio-Laranga, J.; Coret-Ferrer, F.; Casanova-Estruch, B.; Burgal, M.; García-Horsman, J.A. Prolyl oligopeptidase is inhibited in relapsing-remitting multiple sclerosis. *J Neuroinflammation* **2010**, *7*, 23-23

113. Maes, M.; Monteleone, P.; Bencivenga, R.; Goossens, F.; Maj, M.; van West, D.; Bosmans, E.; Scharpe, S. Lower serum activity of prolyl endopeptidase in anorexia and bulimia nervosa. *Psychoneuroendocrinology* **2001**, *26*, 17-26

114. Mantle, D.; Falkous, G.; Ishiura, S.; Blanchard, P.J.; Perry, E.K. Comparison of proline endopeptidase activity in brain tissue from normal cases and cases with Alzheimer's disease, Lewy body dementia, Parkinson's disease and Huntington's disease. *Clin Chim Acta* **1996**, *249*, 129-139

115. Frenssen, F.; Croonenberghs, J.; Van den Steene, H.; Maes, M. Prolyl endopeptidase and dipeptidyl peptidase IV are associated with externalizing and aggressive behaviors in normal and autistic adolescents. *Life Sci* **2015**, *136*, 157-162

116. Crackower, M.A.; Sarao, R.; Oudit, G.Y.; Yagil, C.; Kozieradzki, I.; Scanga, S.E.; Oliveira-dos-Santos, A.J.; da Costa, J.; Zhang, L.; Pei, Y.; et al. Angiotensin-converting enzyme 2 is an essential regulator of heart function. *Nature* **2002**, *417*, 822-828

117. Li, W.; Moore, M.J.; Vasilieva, N.; Sui, J.; Wong, S.K.; Berne, M.A.; Somasundaran, M.; Sullivan, J.L.; Luzuriaga, K.; Greenough, T.C.; et al. Angiotensin-converting enzyme 2 is a functional receptor for the SARS coronavirus. *Nature* **2003**, *426*, 450-454

118. Lan, J.; Ge, J.; Yu, J.; Shan, S.; Zhou, H.; Fan, S.; Zhang, Q.; Shi, X.; Wang, Q.; Zhang, L.; et al. Structure of the SARS-CoV-2 spike receptor-binding domain bound to the ACE2 receptor. *Nature* **2020**, *581*, 215-220

119. Checler, F.; Ferro, E.S. Neurolysin: From initial detection to latest advances. *Neurochem Res* **2018**, *43*, 2017-2024

120. Ravee, R.; Mohd Salleh, F.I.; Goh, H.-H. Discovery of digestive enzymes in carnivorous plants with focus on proteases. *PeerJ* **2018**, *6*, e4914-e4914

121. Lee, L.; Zhang, Y.; Ozar, B.; Sensen, C.W.; Schriemer, D.C. Carnivorous nutrition in pitcher plants (*Nepenthes* spp.) via an unusual complement of endogenous enzymes. *J Proteome Res* **2016**, *15*, 3108-3117

122. Zulkapli, M.M.i.; Ab Ghani, N.S.; Ting, T.Y.; Aizat, W.M.; Goh, H.-H. Transcriptomic and Proteomic Analyses of *Nepenthes ampullaria* and *Nepenthes rafflesiana* Reveal Parental Molecular Expression in the Pitchers of Their Hybrid, *Nepenthes* × *hookeriana*. *Front. Plant Sci.* **2021**, *11*,

123. Cecilio, L.A.; Bonatto, M.W. The prevalence of HLA DQ2 and DQ8 in patients with celiac disease, in family and in general population. *Arq Bras Cir Dig* **2015**, *28*, 183-185

124. Sharma, N.; Bhatia, S.; Chunduri, V.; Kaur, S.; Sharma, S.; Kapoor, P.; Kumari, A.; Garg, M. Pathogenesis of celiac disease and other gluten related disorders in wheat and strategies for mitigating them. *Front. Nutr.* **2020**, *7*, 6-6

125. Janssen, G.; Christis, C.; Kooy-Winkelaar, Y.; Edens, L.; Smith, D.; van Veelen, P.; Koning, F. Ineffective degradation of immunogenic gluten epitopes by currently available digestive enzyme supplements. *PloS one* **2015**, *10*, e0128065-e0128065

126. Chen, Y.-S.; Christensen, J.E.; Broadbent, J.R.; Steele, J.L. Identification and characterization of *Lactobacillus helveticus* PepO2, an endopeptidase with post-proline specificity. *Appl Environ Microbiol* **2003**, *69*, 1276-1282

127. Babkova, K.; Korabecny, J.; Soukup, O.; Nepovimova, E.; Jun, D.; Kuca, K. Prolyl oligopeptidase and its role in the organism: attention to the most promising and clinically relevant inhibitors. *Future Med Chem* **2017**, *9*, 1015-1038

128. Lawandi, J.; Gerber-Lemaire, S.; Juillerat-Jeanneret, L.; Moitessier, N. Inhibitors of prolyl oligopeptidases for the therapy of human diseases: defining diseases and inhibitors. *J Med Chem* **2010**, *53*, 3423-3438

129. Karamyan, V.T. Peptidase neurolysin is an endogenous cerebroprotective mechanism in acute neurodegenerative disorders. *Med Hypotheses* **2019**, *131*, 109309-109309

130. Acharya, K.R.; Sturrock, E.D.; Riordan, J.F.; Ehlers, M.R.W. Ace revisited: a new target for structure-based drug design. *Nat Rev Drug Discov* **2003**, *2*, 891-902

 doi:10.20944/preprints202204.0097.v1

131. Ge, S.; Lu, J.; Hou, Y.; Lv, Y.; Wang, C.; He, H. Azelastine inhibits viropexis of SARS-CoV-2 spike pseudovirus by binding to SARS-CoV-2 entry receptor ACE2. *Virology* **2021**, *560*, 110-115

132. Bastos, I.M.D.; Grellier, P.; Martins, N.F.; Cadavid-Restrepo, G.; de Souza-Ault, M.R.; Augustyns, K.; Teixeira, A.R.L.; Schrével, J.; Maigret, B.; da Silveira, J.F.; et al. Molecular, functional and structural properties of the prolyl oligopeptidase of *Trypanosoma cruzi* (POP Tc80), which is required for parasite entry into mammalian cells. *Biochem J* **2005**, *388*, 29-38

133. Dau, T.; Bartolomucci, G.; Rappsilber, J. Proteomics using protease alternatives to trypsin benefits from sequential digestion with trypsin. *Anal. Chem.* **2020**, *92*, 9523-9527

134. Tsiatsiani, L.; Akeroyd, M.; Olsthoorn, M.; Heck, A.J.R. *Aspergillus niger* prolyl endoprotease for hydrogen–deuterium exchange mass spectrometry and protein structural studies. *Anal. Chem.* **2017**, *89*, 7966-7973